

**Size-segregated Concentration of Bacterial Aerosols in Response to
the Variation of Synoptic Weather at Japan Southwestern Coast**

Chunlan FAN

A dissertation submitted in partial fulfillment of the requirements for the degree of
Doctor of Philosophy

Atmospheric Environment Research Laboratory
Graduate School of Environmental and Symbiotic Sciences
Prefectural University of Kumamoto

February 2023

Supervisory Committee:

Prof. Daizhou ZHANG, Chair

Prof. Yasuhiro ISHIBASHI

Prof. Hiromi MATSUSAKI

Abstract

Bacterial aerosols, i.e., aerosol particles containing bacterial components and ranging from 0.1 μm to 100 μm , are an indispensable part of atmospheric aerosols and widely spreading in the global atmosphere. They play essential roles in the evolution and development of the Earth's environment, although they are also causing big concerns of public health. Quantification of their size-segregated concentration will largely benefit the understandings on their dynamics involved in aerosol variation and dispersion, as well as the roles they play in the complex atmospheric processes and the linking multiple ecosystems. However, the information of the number size distribution of bacterial aerosols is very limited, mainly because the traditional approaches using size-segregated samplers, i.e., Andersen samplers, have unquantified uncertainties, and new technologies rarely provide the accurate concentration of bioaerosols in a wide size range.

In order to establish a reliable method to measure the size-segregated characteristics of bacterial aerosols, laboratory suspension experiments were designed and conducted to assess the uncertainties in the measurements of size-segregated concentration of bacteria-containing bioaerosols with Andersen samplers. The uncertainties were caused by the prolonged impaction time from minutes to hours and even days. Microbes trapped in upper-stage filters in samplers may drop to subsequent-stage filters during the sample collection, leading to supposed uncertainties in the microbial size distribution. This study investigated the uncertainties in bacterial cell number size distribution measured with 8-stage Andersen samplers at a flow rate of 28.3 L min^{-1} (50% cutoff diameters: >11, 7.0, 4.7, 3.3, 2.1, 1.1, 0.65 and 0.43 μm). Results show that the concentration of bacterial cells in the size range of > 4.7 μm could be underestimated 40 - 50% as the concentration in the size range smaller than 3.3 μm was overestimated when the sample collection time was more than 6 hours. Sample collection time should be less than 20 minutes to suppress the uncertainty below 10%, and 42 minutes below 20%. Based on identified exponential inverse relations between the dropping rates and the sample collection time from each stage, a scheme was developed and validated to calibrate the counting results of Andersen sampler samples to obtain the number size distribution of airborne bacterial cells.

Using the calibration scheme, the number size distribution of bacterial aerosols was measured with the same type Andersen samples at AERU (32.324°N, 129.993°E, 23m a.s.l), a coastal site in Amakusa, Kumamoto, southwestern Japan. Results show that the distribution differed according to the source areas: terrestrial air, oceanic air, or a combination of the two. The distribution in the long-distance transported terrestrial air from the Asian continent was

monomodal, with a peak of 3.3 - 4.7 μm . The distribution in local land breeze air was bimodal, with the peaks at 0.43 - 1.1 and 3.3 - 4.7 μm . A similar bimodal distribution was encountered when the local island air and long-distance transported terrestrial air mixed. In contrast, the size distribution did not show clear peaks in the air from either nearby or remote marine areas. According to the air mass backward trajectories, the longer the distance the air moved in the 72 h before arriving at the site, the lower the concentration of total bacterial aerosols. The estimation of dry deposition fluxes of bacterial cells showed that the deposition was dominated by cells larger than 1.1 μm with a relative contribution from 70.5% to 93.7%, except for the local land breeze cases, where the contributions in the size range larger and smaller than 1.1 μm were similar. These results show the distinctive number size distributions and removal processes of bacterial aerosols in different types of air.

Besides, the abundance and viability of particle-attached and free-floating bacteria in dusty air were also quantitatively investigated. We researched this subject based on the fact that airborne bacterial cells are approximately 1 μm or smaller in aerodynamic diameter; therefore, particle-attached bacteria should occur in aerosol samples of particles larger than 1 μm , and free-floating bacteria should occur among particles smaller than 1 μm . Our observations at the AERU, when the westerlies frequently transported dust from the Asian continent, revealed that particle-attached bacteria in dust episodes, at the concentration of $3.2 \pm 2.1 \times 10^5$ cells m^{-3} on average, occupied 72 ± 9 % of the total bacteria. In contrast, the fraction was 56 ± 17 % during nondust periods and the concentration was $1.1 \pm 0.7 \times 10^5$ cells m^{-3} . The viability, defined as the ratio of viable cells to total cells, of particle-attached bacteria was 69 ± 19 % in dust episodes and 60 ± 22 % during nondust periods on average, both of which were considerably lower than the viabilities of free-floating bacteria (about 87 %) under either dusty or nondust conditions. The present cases suggest that dust particles carried substantial amounts of bacteria on their surfaces, more than half of which were viable, and spread these bacteria through the atmosphere. This implies that dust and bacteria have important roles as internally mixed assemblages in cloud formation and in linking geographically isolated microbial communities, as well as possibly have synergistic impact on human health.

In summary, we developed a calibration scheme for the use of Andersen samplers in studies of bacterial aerosols and proposed a guideline, reported the size-segregated concentrations of bacterial aerosols under various weather conditions at Japan southwestern coast, and quantified the particle-attached and free-floating bacteria in dust and nondusty air from the Asian continent.

Keywords: Bacterial aerosols; Anderson sampler; Size range; Distribution mode; Air flow; Bacterial deposition

Content

Abstract	I
Chapter 1 Introduction	1
1.1 Bacterial aerosols in the atmosphere	2
1.2 Roles and spreading in the atmosphere	4
1.2.1 Atmospheric reaction	5
1.2.2 Aerial transportation	6
1.2.3 Deposition	8
1.3 Detection techniques	10
1.3.1 Traditional impactors	10
1.3.2 Real-time sensor measurement	12
1.4 Current understandings	13
1.4.1 Understandings in impactor observations	13
1.4.2 Understandings in real-time observations	14
1.5 Research objectives and contents	15
Chapter 2 Calibration for number size distribution of bacterial cells measured with traditional size-segregated aerosol samplers	17
2.1 Introduction	18
2.2 Methodology	19
2.2.1 Suspension in clean hood	19
2.2.2 The preparation of filters	20
2.2.3 Identification of bacterial cells	21
2.2.4 Dropping rate and transfer coefficient	21
2.2.5 Calibration equation	22
2.3 Results	23
2.3.1 Concentration and size distribution with and without the suspension	23

2.3.2	Variation of dropping rates according to size ranges	24
2.3.3	Dependence of dropping rates on suspension time	25
2.4	Application examples	28
2.5	Discussion	29
2.6	Summary	31
Chapter 3	Number size distribution of bacterial aerosols in terrestrial and marine airflows at a coastal site of Japan	32
3.1	Introduction	33
3.2	Materials and methods	33
3.2.1	Sample collection	33
3.2.2	Backward trajectories and meteorological conditions	34
3.2.3	Categories of samples in terms of potential sources	35
3.2.4	Enumeration and calibration	37
3.2.5	Dry deposition estimation	38
3.3	Results	39
3.3.1	Distribution in the long-distance transported terrestrial and marine air	39
3.3.2	Distribution in the local land and sea breeze air	41
3.3.3	Distribution in mixed air	43
3.3.4	Estimated dry deposition fluxes	44
3.4	Discussion	45
3.4.1	Factors determining monomodal and bimodal distributions	45
3.4.2	Activation and removal of the bacterial cells in size ranges	47
3.5	Summary	48
Chapter 4	Abundance and viability of particle-attached and free-floating bacteria in dusty and nondust air	50
4.1	Introduction	51
4.2	Methods	51

4.2.1	Sample collection and cell enumeration	51
4.2.2	Separation of particle-attached and free-floating bacteria	53
4.2.3	Atmospheric conditions	58
4.3	Results	58
4.3.1	Concentrations of airborne bacteria in segregated size ranges	58
4.3.2	Concentration of particle-attached and free-floating bacteria	60
4.3.3	Viabilities of particle-attached and free-floating bacteria	63
4.4	Discussion	64
4.4.1	Implication from the comparison with literature data	64
4.4.2	Ice cloud formation.....	65
4.4.3	Ecosystem conservation and development.....	65
4.4.4	Health effects.....	66
4.5	Conclusions	67
Chapter 5	Conclusions and perspectives	68
	Acknowledgements.....	71
	References	72

Chapter 1 Introduction

1.1 Bacterial aerosols in the atmosphere

Bioaerosols are airborne particles of biological components including fungi, bacteria, viruses, pollen, and metabolic fragments such as endotoxins, mycotoxins, and glucans (Cox and Wathes 1995).

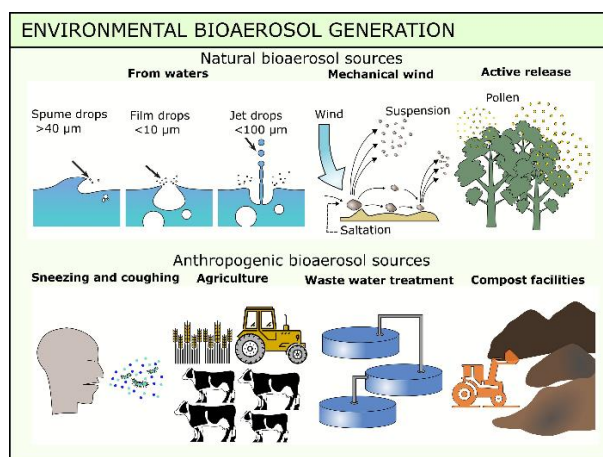


Figure 1-1 Schematic of bioaerosol generation mechanism. Reprinted from Alsved et al. (2020)

As shown in Figure 1-1, bioaerosols are generated from natural and anthropogenic sources. In nature, aquatic surface, plant release, and animal activities are the major sources which emit abundant bioaerosols into the atmosphere (Xu et al., 2011). The relative importance of these sources varies with altitude, season, location, and meteorological factors in general. In most terrestrial environments the main providers of bacteria in the near-surface atmosphere are plants (i.e., leaf surfaces) and soil (Bowers et al., 2013). The global leaf surface area is estimated to be approximately four times the terrestrial ground surface area. As for human activities, agricultural activities, wastewater treatment plants, and composting are common sources. The type of aerosol source plays a role in the various characteristics of the bioaerosols released. In particular, it affects the size of airborne microorganisms and their residence time in the air. According to Burrows et al. (2013), the residence time of bacteria may be shorter for bacteria emitted from the ocean than for bacteria emitted from land surfaces, because of more rapid removal by precipitation. Moreover, consistent with the smaller size of marine bacteria, the median count diameter of particles associated with culturable bacteria has been found to be smaller at coastal sites (around 2 μm) than at continental sites (about 4 μm).

Figure 1-2 shows the size characteristics of bioaerosols of various components, with the size ranging from 0.001 nm to 100 μm. The size is closely related to the sources. Small particle

is more effective to spread leading to their higher concentration in the atmosphere in comparison with large particles size. Among various components of bioaerosols, bacteria are predominant and constitute 80% of total bioaerosols (Gao et al., 2014). Bacteria are unicellular prokaryotic microorganisms, i.e., a single-celled organism is lack of a membrane-bound nucleus or organelles. They have various shapes from spherical coccoid cells to thin or thicker rods. Cell diameter is typically around 1 μm , as ultrasmall cells $<0.1 \mu\text{m}$ in diameter exist in some species (Miteva and Brenchley, 2005). Bacterial aerosols are air-suspended particles of soil dust or organic aggregates with bacteria attached. They exist in wide size ranges. Some species of bacteria (*Bacillus spp.*, most notably) can form spores to resist extreme conditions (temperature, desiccation, ultraviolet, oxidation, chemical assault), allowing survival in long-distance transportation with airflows (Smith et al., 2012b). Therefore, it is crucial to have knowledge about the properties and characterization of bacterial aerosols in terms of specifically dispersion mechanism, and eventually implicate and model the atmospheric processes.

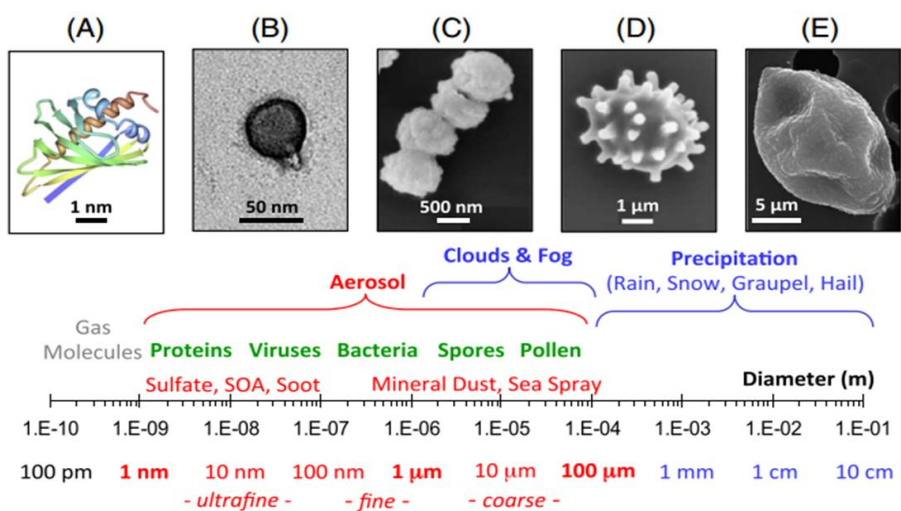


Figure 1-2 The size distribution of bioaerosols with exemplary illustrations: (A) protein, (B) virus, (C) bacteria, (D) fungal spore, and (E) pollen grain (Fröhlich-Nowoisky et al., 2016).

In the atmosphere on the global scale, the total number of bacteria aloft within the first 3 km of altitude was estimated to be around $\sim 10^{19}$ (Whitman et al., 1998). In general, the concentration of bacterial aerosols near the ground ranges from $\sim 10^2$ to $\sim 10^6$ cells m^{-3} (Bowers et al., 2013; Fang et al., 2007; Harrison et al., 2005). Bacterial aerosol vary apparently in number and composition, showing diurnal and seasonal patterns: higher concentration during the warm periods of the year than in winter, and higher during daytime compared with nighttime which are

recognized as the consequence of the upward fluxes lofting cells from surfaces (Bowers et al., 2012; Bowers et al., 2011; Franzetti et al., 2011; Fröhlich-Nowoisky et al., 2014a).

Aloft for typically 2–10 days, bacteria cells can travel over thousands of kilometers (Murata and Zhang, 2014; Smith et al., 2012a). Living specimens were recovered from altitudes of several tens of kilometers above ground level. This phenomenon attests to the high resistance of certain species or strains to cold, ultraviolet, and other stresses in the atmosphere (Joly et al., 2015). Many outdoors airborne bacteria originate from plants and soils (Bowers et al., 2013; Maron et al., 2005), where they probably acquired some level of adaptation to atmospheric stresses. However, the vision of the biodiversity differs from one study to another, partly due to differences in methods.

The generation, dissemination, and deposition of the bioaerosols are dependent on their characteristics (e.g., size, density, shape), local weather (e.g., atmospheric relative humidity, temperature) and airflow (e.g., source, transporting distance). So far, the patterns of biodiversity in the airborne bacteria appear very variable and have rarely been linked to environmental variation. The influence of meteorological factors (wind speed, humidity, or temperature) on bacteria abundance in the air has been reported in several studies (Harrison et al., 2005; Lighthart et al., 1971), but more evidence is needed to clarify the relation between synoptic weather and bacterial aerosols.

The variations of bacterial aerosols contribute differently to the development, evolution, and dynamics of ecosystems. Their dispersion within the atmosphere from various sources such as human, plant and animal and has a potential impact on environment and human health. Bioaerosols assist the formation of cloud droplets (Ariya et al., 2009a), ice crystals (Schnell and Vali, 1976), and acts as regulating media of precipitation especially in pristine air, thereby influencing the hydrological cycle and the climatic instabilities (Ariya et al., 2015). In case of marine ecology, biological particulate matters significantly contribute to the ice nuclei (Fröhlich-Nowoisky et al., 2016). Thus, bioaerosols plays an indispensable role in the transportation of microorganisms, promote the interchange of genetic, and support geographical shift between the habitats and biomes.

1.2 Roles and spreading in the atmosphere

Over the past several decades, attentions have been paid to bacterial aerosol research from various aspects for their important roles in environmental processes, such as cloud formation (Smets et al., 2016), atmospheric chemical reactions (Fröhlich-Nowoisky et al., 2016), and links

between independent biomes.

1.2.1 Atmospheric reaction

Bacterial aerosols could take part in the formation of clouds by acting as ice nuclei (IN), which determine the cloud formation and precipitation. Ice nucleation in cloud droplets occurs either via the freezing of water already condensed around a particle, by water vapor condensing and simultaneously freezing onto a particle, or by a particle contacting a supercooled droplet. Metabolically active bacteria in clouds have been investigated regarding their potential impacts on cloud formation. Bacterial concentrations in cloud droplets reach concentrations of around 10^5 cell ml⁻¹ (Amato et al., 2017). A research revealed that nearly 20% of bacteria were potential IN species in the profile of bacteria present in aerosol downwind during corn harvesting periods in Nebraska (Garcia et al., 2012), but sequencing of IN genes, which code for the active protein, revealed that *Pantoea agglomerans*, which accounted for 11% of all bacterial sequences, was the primary IN species. It is commonly stated that mineral dusts are the major source of ice nucleating particles (INPs) at temperatures colder than about -20°C , whereas particles of biological origin may dominate atmospheric INPs above about -15°C (DeMott and Prenni, 2010; Morris et al., 2014). While the known IN bacteria are enriched in rainfall compared with cloud water (Joly et al., 2013), and released by the action of rainfall and harvesting (Constantinidou et al., 1990). Similar pattern was found in fresh snow (Hill et al., 2014), but IN bacterial aerosols tend to have more significant impact in the formation of thunderstorm hail (Michaud et al., 2014). The concentration of IN bacteria in air at cloud height can be estimated from their abundance in precipitation by assuming to be 0.4 g of condensed water of 1 m³ of cloud contains (Michaud et al., 2014).

The present of bacteria in atmosphere could also take part in some chemical reactions. Bacteria capacities to survive in clouds generally keep metabolically active. Amato et al. (2005) detected numerous bacteria isolated from clouds at a high-altitude station (France) for their ability to transform methanol and formaldehyde. Results showed that all of the bacterial strains detected actively degraded formaldehyde, while distinctive reactions were observed for the transformation of methanol: Gram-positive bacteria mainly degraded methanol, Gram-negative bacteria degraded but mainly produced methanol. In addition, Vařtilingom et al. (2013) clarified that the microbial community present in real cloud samples can fully degrade formaldehyde. Interestingly, it was shown that decreasing the temperature of incubation from 17°C to 5°C has little impact on the biodegradation rates of four different strains isolated from clouds (two *Pseudomonas sp.*,

Bacillus sp., and *Frigoribacterium sp.*). Hill et al. (2014) also showed that 76% of all bacteria remain alive in cloud water, by a staining method of redox dye. In terms of monocarboxylic acids, Herlihy et al. (1987) were the first to study the degradation of formic and acetic acids by bacteria in rainwater. Amato (2012) showed that 60 microbial strains present in cloud water are able to transform formic, acetic, and lactic acids. This study was performed at 27°C using pure cultures with one single substrate in phosphate buffer.

In addition, studies have shown that microorganisms isolated from clouds and rainwater can produce biosurfactants. Ahern et al. (2007) showed that 70 fluorescent *Pseudomonas* isolates are biosurfactant producers, with 43 constituting high producers. This work highlights the importance of bacterial strains to atmospheric waters as the main group encountered and as the more active group in terms of biosurfactant production. While the presence of biosurfactants in cloud water has not yet been proven, they have been found in atmospheric aerosols. Few mechanisms have been presented in the publications, and these mechanisms must be evaluated through cloud chemistry models. Research on biological contributions to the production of these compounds is at its infancy. The biotransformation of biogenic substrates should be investigated in greater detail in reference to particular amino acids.

1.2.2 Aerial transportation

Bacterial cells, either individually or particle-attached, move via airflows at different scales. It is higher possibility for bacteria to spread globally than fungi or pollens due to their smaller size, leading to higher chance for microbiological communication among various ecosystems. First, aerial transport and subsequent deposition can deliver microorganisms to any type of distant surface that is exposed to the air. The viability of bacteria during dust transportation to the downwind environment is likely to be 16 – 40%, which was lower than in non-dusty air; however, the viable cell concentrations of bacterial aerosols in dust, were similar to those in non-dusty air (Hara and Zhang, 2012). Second, survival under the environmental conditions that accompany such a voyage often requires a physiological state that is near or bona fide dormancy. The interaction of wind with aquatic and terrestrial surfaces is a main route to emit bacterial aerosols allowing for their entrainment into air masses that can be transported regionally and globally. Near surface interactions between urban waterways and urban air have been well studied but some level of interaction among these bacterial communities would be expected and may be relevant to understanding both urban air and water quality.

For aerial transport, there is increasing evidence showing the long-distance transport

capability and pathways of bioaerosols. Successful invasion of microorganisms immigrating via the atmosphere occurs under rather survival through special conditions in the new habitat, or the capacity of the disseminating particle to avoid the dormant-like state through association with a protective particle during transport. There are example studies of cases where airborne microorganisms successfully establish in, and sometimes invade a new habitat, and subsequently lead to the consequences for ecosystem functions and microbial evolution. In Asia, bacterial aerosols are frequently observed being transported along with dust during Asian dust events. The transit of air masses over the continental and marine surfaces has been observed to be selective for some bacterial taxa. Field observations have shown that natural desert dust and anthropogenic pollution are efficient vectors for carrying bacterial aerosols from the Asian continent downwind (Maki et al., 2013; Maki et al., 2017). *Actinobacteria* was significantly abundant and marine bacterial signatures were more prevalent when the air was influenced dominantly by the Sea of Japan (Maki et al., 2019). Air masses from oceanic sources had higher relative abundance of diversity in common with the coral dataset (8.8%) compared to air with recent continental transit (2.2%) at the Great Barrier Reef (Archer et al., 2020). Presumptive ice nuclei bacterial species, including *Bacillus atrophaeus*, detected in North America were found to originate from China or Japan and had taken approximately 10 days to travel across the Pacific Ocean in the free troposphere (Smith et al., 2012; Smith et al., 2013). Therefore, once entering free troposphere, bacterial aerosols are no longer submitted to the intense mixing of the planetary boundary layer, so that light enough particles then have the potential to travel over very long distances, on continental or trans-oceanic scales, under the action of trade winds for instance or dust storms (Prospero et al., 2005).

Bacterial aerosols in transport pathway vary substantially according to their size. A recent modeling study demonstrated that such potential should become increasingly unlikely for particles greater than 20 μm in diameter (Wilkinson et al., 2012), and virtually impossible for particles larger than 60 μm . Bacterial aerosols, shown by Yamaguchi et al. (2014) and Prospero et al. (2005) to have traveled over very long distances, were indeed smaller than 20 μm ; however, pollen grains between 20 and 80 μm were found in Greenland, with an estimated average transport duration of 5 days. Size-differentiated bacterial aerosols participate in various processes associated with atmospheric aerosol particles. *Pseudomonas syringae* is a well-known species that produces ice nucleation proteins and can promote nucleation for ice cloud formation (Monteil et al., 2014; Stopelli et al., 2017). A single cell of *P. syringae* is approximately 0.7 μm , and its aggregation is frequently as large as 2 μm (Alsved et al., 2018). Fine particles, such as individual

cells, are easily uplifted into clouds and eventually incorporated into cloud droplets. In contrast, coarse particles such as particle-attached cells would have shorter upward trajectories on average, and many tend to be washed out by raindrops in below-cloud air (Monteil et al., 2014).

1.2.3 Deposition

Airborne bacterial aerosols are removed by deposition, including wet deposition (i.e. rainfall, hail and snowfall) and dry deposition. For dry deposition to the recipient environment, which is a dominant and continuous process whereby bacterial aerosols settle or collide and stick onto downwind surfaces, promoting the genetic import. It is usually quantified through a deposition velocity, expressed as the ratio of the downward particle flux, and related to the ambient particle concentration.

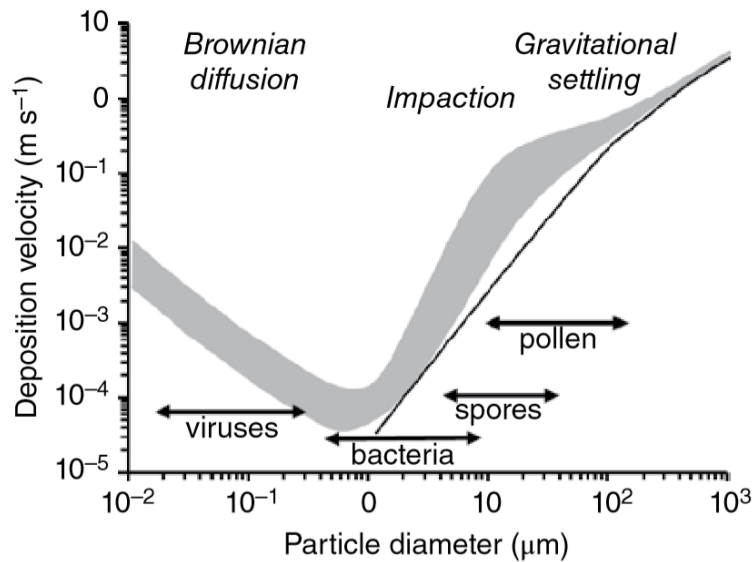


Figure 1-3 Dry deposition velocity and aerodynamic particle diameter, after the single-layer surface model of Raupach and Berne (2015). The case represented here is for a vegetation of height 0.06 m and leaf area index 1. The shaded area shows the range of deposition velocities calculated for a range of wind speeds giving friction velocities between 0.35 and 1.40 m s^{-1} . The solid line is the predicted terminal velocity. Diameter ranges for four types of bioaerosols are shown.

Three main mechanisms are involved in determining dry deposition of bacterial aerosols on terrestrial surfaces: gravitational settlement, inertial impaction on individual elements, and Brownian diffusion through the boundary layers attached to each element. Each of the processes

is a strong function of the particle aerodynamic diameter: Brownian diffusion for submicrometer particles and gravitational settling for large particles, basically above 100 μm . Particles size at around 10 μm settle in governance of impaction. The combination of these processes results in a “V-shaped” curve exhibiting a minimum at around 1 μm , where none of these processes is effective. The deposition of bioaerosols therefore depends to a large extent on their type: bacterial fragments are in the submicrometer range where diffusion is the main deposition mechanism, whereas bacteria attached to particles are in the ascending branch and are strongly subjected to gravity forces. Most bacterial are in the size range of minimum deposition velocity, indicating the potential to be dispersed by wind over large distances; and mainly settled down by washout. It has indeed been shown that bacteria can remain aloft for between 5 and 10 days typically, in cloud-free conditions, but for a much shorter time when condensed water is present (Burrows et al., 2009a). However, this applies to single bacterial cells, but in reality bacteria are often aggregated, or attached to dust particles or small vegetation fragments, so that their mean aerodynamic diameter is larger (e.g., 4 μm , as found at various continental sites (Shaffer and Lighthart, 1997). The deposition velocity is instead at the start of the ascending branch on the right-hand side of the curve.

The dependency of deposition velocity on particle size also has consequences to particle segregation during transport. It has been demonstrated that the particle size after emission tends to decrease with distance from the sources. This is because of the preferential deposition of large particles close to the source areas by the effect of gravity (Fuzzi et al., 1997). Bacterial aerosols may evaporate and shrink during their journey and remain aerial for longer time. The deposition velocity is often expressed as the inverse of a sum of resistances, using an electrical analogy. Its parameterization is based on surface models of varying complexity. For instance, Raupach and Berne (2015) used a single-layer model for vegetated surfaces, and Petroff et al. (2000) elaborated a model for deposition velocity over plant canopies with significant vertical extent. The terminal velocity, i.e., the settling velocity under the sole action of gravity in still air, is described approximated by Stokes law and in a linear variation with the square of the diameter.

Lower deposition velocity may partly result from the possibility that particles will be lifted into the planetary boundary layer, depending on their size, weight, and density, as well as on the intensity of convective motions. During convective conditions, the settling velocity of particles are 3×10^{-1} , 3×10^{-3} , and $3 \times 10^{-5} \text{ m s}^{-1}$ for particle diameter of 100 μm , 10 μm , and 1 μm , respectively, in the Stokes regime), making it clear that even larger particles such as pollen grains can be lifted to heights above the stable boundary layer. The presence of numerous biological

aerosols in the planetary boundary layer has indeed been demonstrated using light aircraft (Raynor et al., 1974) as well as unmanned aerial vehicles (Aylor, 1986). Aerial measurements performed by Lin et al. (2014) on fungi in the genus *Fusarium* have been used to deduce distances to the potential inoculum sources ($\approx 1-4$ km), as well as their seasonal variations. Smaller particles with a small deposition velocity such as bacteria: for instance, Mandrioli et al. (1984) found from aircraft measurements that much more abundant concentration of bacterial aerosols above the planetary boundary layer (at about 6000 and 3000 m, respectively) than pollen and spores.

Substantially, the atmospheric reaction, cloud formation, flying time, and deposition ability of bacterial aerosols are involved in their size, leading to the importance of quantification of size distribution of bacterial aerosols.

1.3 Detection techniques

Various samplers have been developed for identification of size-segregated bacterial aerosol, because size distribution of bacterial aerosols is essential for their promotion in various aspects, and the main categories for this type of samplers are traditional impactor and real-time fluorescent measurement.

1.3.1 Traditional impactors

Aerodynamic size refers to the diameter of a spherical particle of unit density with the same gravitational settling velocity as the particle under consideration, which is necessary to define the behavior of aerosol-related processes. Impactor samplers are designed to collect the bioaerosols. So far, the most widely-used size-segregated impactor is the Andersen multistage impactor, which was introduced in 1958 (Andersen, 1958). It has been recommended and used as a reference sampler (Griffin et al., 2001; Yao and Mainelis, 2007) and is the recommended bioaerosol collection method in the NIOSH Manual of Analytical Methods (Jensen and Schafer, 1998) (NIOSH 2017). An impaction sampler is to collect the bacterial aerosols from air and force them to change direction, causing the particles with high inertia to collide with the collecting surface (Henningson and Ahlberg, 1994). In general, particles of larger size settled on the surface, and the smaller ones more easily pass the stage in the airstream without collision. The samplers are characterized by their inlet size, shape, collection chamber, impaction surface, which can be solid (glass slide), semi-solid (agar), or gelatin (Macher and Hansson, 1987). The collection and recovery rates are correlated to the velocities of air jets. Moreover, sampling duration and impaction velocity are important factors in the collection and viability of bacterial aerosols. The

use of the semi-solid surfaces, such as agar plates, has been shown to have more flaws due to the overlap of the collected microorganism colonies on one another, making particle differentiation difficult (Feller, 1991). Desiccation issues are becoming an increasing challenge in sampling because the surface moisture is removed by air stream passing over the agar plate, limiting the ability to impact more particles due to reduced sticky nature of the surface (Cox and Wathes, 1995). Despite the numerous disadvantages, the advantages of impaction technology are its easiness to use and low cost. The cascade impactor, slit sampler, stacked sieve six stage Anderson variable impactor, and Rotorod sampler have all proven their worth in the collection efficiency of various airborne microorganisms.

One of the main advantages of using impactors to collect airborne microorganisms, especially culturable ones, is the easiness of use and convenience: once a sample is collected, the agar plates are transferred directly to an incubator without intermediate steps. Agar is not designed to use with analytical methods other than culturing, although attempts have been made to scrape off the deposited microorganisms using water and analyze them using PCR (Xu and Yao., 2011). In addition, impaction subjects airborne microorganisms to sudden deceleration and that damages them, including the loss of culturability and even membrane integrity (Chen et al., 2005) thus further reducing the fraction of culturable microorganisms that can be determined. Nonetheless, the convenience of use and a large amount of reference information make agar-based impactors a tool of choice in many studies. Culturable methods are essential to determine the viability and proliferation ability of microorganisms, but they constitute only a fraction of 1-6% in total microorganisms (Rinsoz et al., 2008) and neglect viable but not culturable microorganisms, and non-viable microorganisms which could still lead to various effects (Speight et al., 1997). Therefore, other media such as different types of filters are applied to Andersen sampler to collect the total of culturable, non-culturable, viable, and non-viable bacterial aerosols.

Polycarbonate, mixed cellulose ester, polytetrafluoroethylene, polyvinyl chloride, nylon, gelatin, and other filter types have been used for bioaerosol sampling applying with the size-segregated impactor to catch the bioaerosols according to their cut-off size (Burton, Grinshpun, and Reponen 2007; Li et al. 2018; Van Droogenbroeck et al. 2009). When using flat filters, particles are collected on the membrane surface, which is especially conducive for microscopy analysis (Crook, 1995). Washable filters have also been used (Choi et al. 2018). Once the bioaerosol particles are collected on a filter, they can be eluted into liquid for subsequent analysis by various techniques. Particles deposited on a filter can also be examined directly using microscopy, including electron microscopy or be directly placed directly on agar for cultivation.

After collecting the particles on to the glass slides with a semisolid media and filters attached to samplers, the particles including bacterial aerosols on the media can be processed for cell concentration, viability, morphology, community structure, etc.

However, the applicability of this approach remains unknown for long-term integrated samples and detection uncertainties. The pore size and collection substrate of these filters, as well as operating time and the collected air volume may not be known unless specifically measured. In particular, the collection duration by filters can be extended to several hours and even months, which could affect the collection's certainties, leading to the quantification of bioaerosol size distribution even more challenging.

1.3.2 Real-time sensor measurement

Real-time Polymerase Chain Reaction (RT-PCR), a real-time sensing approach for accurate measurement of microorganisms in the environment, which employs a thermo cycler coupled to an optical module that measures the intensity of the reactions using hybridized probes and double-stranded deoxyribo nucleic acid (DNA) dyes (Stetzenbach et al., 2004). Metagenomics aids in the genomic analysis of uncultured samples collected from the environment. The procedure consists of three steps: isolation of DNA (Stein et al., 1996), cloning of DNA into a suitable vector, and transferred to host bacterium (Lorenz et al., 2002). Further, shotgun is the most commonly used device for metagenomics analysis, which uses computational power to generate a clone library (Zaghdoudi et al., 2013). Thus, the high throughput sequencing technologies such as shotgun metagenomics not only provide information, but also the metabolic process in the community.

The fluorescence aerodynamic particle sizer (FLAPS) instrument, whose development was commissioned by the Canadian Department of National Defense at Suffield, and was to assess the feasibility of single-particle fluorescence sensing for live biological threat agent detection. Particle sizer is with a 354 nm laser added to excite fluorescence of the sized particles (Kaye et al., 2005). Particle sizing is provided as an function which convolves the particle shape, density, and size (Huffman et al., 2010), and is achieved by measuring the particle time of flight between two red He and Ne lasers at 633 nm (Hairston et al., 1997). The size of each particle is recorded in one of 52 logarithmically spaced size bins, or alternatively into one of 30 linearly spaced bins (Huffman et al., 2010). The instrument has typically been reported to reliably size particles of 0.5–15 μm , although the manual for the commercially available states an upper range of 20 μm . One benefit of the UV-APS is that the aerodynamic size generally allows the instrument to provide a more narrowly resolved particle size measurement than instruments that detect size

optically. In addition to the aerodynamic size and fluorescence intensity, the intensity of light scattered by the near- infrared sizing beams are also recorded and in principle can be used as a measure of optical diameter; however, data are only recorded as ensemble distributions of particle size and fluorescence over a user-defined period (minimum 1 s). This limits the ability of a user to compare aerodynamic and optical size for discrete particles. Without the ability to investigate and compare the properties of individual particles, the broad applicability of the UV-APS for continuous measurements of ambient aerosol is significantly diminished.

Overall, real-time sensor measurements can analyze the size distribution of bacterial aerosols at high time-resolution for continuous observation. However, these techniques are only accessible for a few researchers due to the expensiveness, higher technical threshold, and patent limitation.

1.4 Current understandings

Airborne primary biological particles are thought to represent as much as 25% of the total number concentrations for particles larger than 0.2 μm (Jaenicke, 2005), and numerous studies were conducted to investigate more detailed information of the size distribution of bacterial aerosols. As mentioned above, the main sampling techniques to quantify the size distribution are off-line size-segregated impactors and on-line ultraviolet aerodynamic particle sizer.

1.4.1 Understandings in impactor observations

Traditional size-segregated impactor Andersen samplers can collect bacterial aerosols according to their size ranges, and nutrient agar is the conventional media to quantify the culturable colonies of bacterial aerosols. The aerodynamic diameter of bacterial aerosols is firstly involved in the transmission of airborne pathogens of concern to human, animal or plant health depend on the ability of the microorganisms to cause infection and, subsequently, disease when interacting with a host. The aerodynamic diameters of bacterial aerosol particles govern their distance of spread and infiltration into the human respiratory system, implying different health risks from microbial inhalation (Yao, 2018). Much attention has been paid to the size distribution of bioaerosols, as it is closely related to their deposition efficiency and subsidence area (Fan et al., 2019; Ferguson et al., 2021; Gong et al., 2020; Yang et al., 2021; Yin et al., 2021). Bacteria were found to exist mainly in coarse particles ($> 2 \mu\text{m}$) (Bowers et al., 2013; Cao et al., 2014; Gong et al., 2020). In addition, bacteria presented distinctive size distribution pattern among different regions. For example, unimodal patterns were attained for total airborne microorganisms in hazy days with a peak of 2.1-3.3 μm in an inland populated city in western China during hazy

episodes (Yang et al., 2021). In contrast, a bimodal size distribution of airborne bacteria was observed with two peaks, 1.1 - 2.1 μm , and 4.7 - 7 μm in the coastal Qingdao in eastern China (Yin et al., 2021). Inhalation is the major route for microbial pathogens to enter human respiratory systems. Adverse reactions can harm both the upper and lower respiratory tract. Inhalable bacteria aerosols with a diameter of $< 4.7 \mu\text{m}$ can penetrate into the lower respiratory system (Nasir et al., 2012) and elicit allergic or inflammatory responses (Smets et al., 2016). Through endotoxins, bacteria aerosol can produce a strong immune response and can cause acute and chronic health effects (Rylander, 2006).

Aerodynamic size of bacterial aerosols is also related to their roles as ice nuclei in cloud formation, and dispersion ability. This ability is a function of a variety of factors (e.g. environmental, microbiological, etc.) which affect the integrity of the airborne microbes. Long-range transport can lead to water evaporation of bacterial cell, which conversely influence to aerosol particle size. During atmospheric transport, bacterial aerosol droplets undergo a series of evaporative and rehydration processes which result in changes in their size-dependent metabolism and physiology.

1.4.2 Understandings in real-time observations

Huffman et al. (2010) used Ultraviolet-Aerodynamic Particle Sizer to show that the concentration and frequency of occurrence of 3 μm fluorescent bacterial fluorescent biological aerosol particles at Mainz, Germany (semi-urban environment), and it exhibited a strong diurnal cycle. Gabey et al. (2010) found that the FBAP in Manchester, UK, follow a characteristic bimodal distribution with peaks at 1.2 and 1.5–3.0 μm . Geometric mean diameters (GMDs) of molecular markers of biomass burning and primary biological aerosols showed that there was no significant difference in the coarse mode ($>2.1 \mu\text{m}$) between the haze and non-haze samples. A size shift towards large particles and large geometric mean diameters in the fine fraction ($<2.1 \mu\text{m}$) was detected during the hazy days. It highlights that the stable meteorological conditions with high relative humidity favor the condensation of organics onto coarse particles (Xu et al., 2020). Preliminary ambient measurements in Mainz (Germany, central Europe) show that an emission peak was frequently observed for fluorescent fine particles (0.5–1 μm). Of all detected particles of $>100 \text{ nm}$ in diameter, 13% by number were identified as primary biological aerosol particles (PBAPs). One type of PBAPs mostly appeared as similar rod-like shapes with an aspect ratio > 1.5 . Size distribution of the rod-like PBAPs displays two typical peaks at 1.4 μm and 3.5 μm ,

which are likely bacterial and fungal particles (Li et al., 2020). It can be concluded from the literatures above that the optical size of airborne biological aerosols are dominant in the size of smaller than 3 μm .

However, the size distribution of bacterial aerosols is still in lack of enough information to strongly support transport dynamical theory, and more investigation is in need to improve the understandings on the aerodynamic characteristics of bacterial aerosols.

1.5 Research objectives and contents

Transport of bacterial aerosols is an efficient link connecting the plausible isolated micro ecosystems on the earth. To further understand the dissemination mechanism of bacterial aerosols in the atmosphere, size-dependent cell concentration, variations in different scale of synoptical weather, and dry deposition flux are essential.

It is important to reveal the size-dependent dynamics of bacterial aerosols behavior via airflows locally, regionally, and even globally, and to influence to receptor environment. The bacterial concentration of all size and their viabilities have been investigated in previous studies. The information of cell number size distribution remains vague. The lack of the knowledge is because there is not validated method to quantify the cell number size distribution even though there are multiple techniques for sample collection. The main objectives of this study are listed as follows:

1. To provide a calibrated scheme to reduce the uncertainties for commonly used size-segregated samplers.
2. To study the number size distribution of bacterial aerosols under various synoptic weather conditions, i.e., the airflow patterns to disseminate bacterial aerosols in the atmosphere.
3. To support better understanding in the role of bacterial aerosols via airflows to link distanced ecosystems.
4. To give insights into the deposition of bacterial aerosols of different size ranges.

The specific research contents in this study include:

1. Based on suspension experiments of collected bacterial aerosol samples, we measured the uncertainties in Andersen sampler by polycarbonate filter, and propose a calibration scheme

aimed at reducing the uncertainties caused by prolonged sampling duration.

2. Using the calibrated method, the number size distribution of bacterial aerosols was obtained and applied to explore the influence of airflow source on size modes of bacterial aerosols.
3. Size-dependent dry deposition of bacterial aerosols was estimated.
4. To compare the particle-attached and free-floating bacteria in the air and the viability of these bacteria under dusty and non-dusty conditions, and quantify the impact of dust periods on status of bacterial aerosols.

Chapter 2

Calibration for number size distribution of bacterial cells measured with traditional size-segregated aerosol samplers

2.1 Introduction

For efficient collection of bioaerosols in a wide size range, bioaerosols samplers with the collection mechanisms of inertial impaction, filtration, liquid impingement, or online laser-excited fluorescence detection are used (Yao, 2018). WIBS is an effective way to detect the number distribution of bioaerosols according to optical diameter, but the aerodynamic diameter is preferred in the investigation of health inhalation and climate impact (Kaye et al., 2005). Many studies made efforts to link optical diameter to aerodynamic diameter, which were unfortunately limited to shapes and the properties of particles (e.g., Chien et al., 2005). Traditional off-line Andersen samplers have been used widely in airborne culturable microorganisms' observation (Dunbar et al., 2005; Xu et al., 2013), owing to their convenience and low expense, mostly in areas of human exposure risk assessment (Manibusan & Mainelis, 2022).

Andersen samplers have been widely used in both indoor and outdoor environments such as hospital, nursery home, urban and coastal air and so on (Gong et al., 2020; Tsay et al., 2020; Yang et al., 2021). The samplers differentiate airborne microorganisms based on their inertial according to the particle aerodynamic size (Andersen, 1958). This type of samplers was invented to collect airborne culturable microorganisms on agar plates within 20 minutes. Culturable microorganisms make up only around 1-6% of the total airborne microorganisms, which are crucial when evaluating human health and climate effects (Durand et al., 2002).

With the development of recent technologies, other typical collection media have been applied to collect airborne microorganisms on stages such as polycarbonate filters, glass fibers, quartz and other types of membranes. Polycarbonate filters were used with a six-stage Andersen sampler by Gong et al. (2020) to investigate the airborne bacterial viability by BacLight live/dead staining method and discussed the health impact from bioaerosols in different size ranges. In this untraditional way, the sampling duration is normally longer than that of conventional petri dishes to get enough quantity for identification, for 30 minutes, a couple of hours, and even one month (Agarwal, 2017; Tanaka et al., 2020; Tang et al., 2021; Woo & Yamamoto, 2020; Yang et al., 2021; Yin et al., 2021)

Hu et al. (2020) found that during prolonged sample collection with Andersen samplers, bacteria trapped by upper stages fell onto lower stages. The dropping was supposed to cause uncertainties in the result of size-segregated bacterial cell concentrations, which were estimated from the cell counts on the filters in the samplers. To better understand the uncertainties by Andersen samplers for culture-independent method and long-time sampling, more investigations

are necessary for the verification of the applicability. In this study, by utilizing 8-stage Andersen cascade impactors, the uncertainties were studied for the concentration of size-segregated bacterial cells due to the dropping from upper stages to lower stages. Factors including bioaerosols size and sampling time were investigated. This study aims to apply quantitative and qualitative analyses to reduce the uncertainties in bacterial aerosols size distribution measured with size-segregated impaction samplers.

In this chapter, suspension experiments were designed and conducted to test the uncertainties of bacterial cell sampling by Andersen sampler. Factors including bacterial aerosols size and sampling time were investigated. It aims to apply quantitative and qualitative analyses to reduce the uncertainties in bacterial aerosols size distribution measured with size-segregated impaction samplers.

2.2 Methodology

2.2.1 Suspension in clean hood

In this study, Andersen samplers (model AN-200, Tokyo Dylec Corp.) were used to collect airborne aerosols, which divide the airborne particles into eight size ranges: $>11\mu\text{m}$ (Stage 0); $7.0\text{--}11\mu\text{m}$ (Stage 1); $4.7\text{--}7.0\mu\text{m}$ (Stage 2); $3.3\text{--}4.7\mu\text{m}$ (Stage 3); $2.1\text{--}3.3\mu\text{m}$ (Stage 4); $1.1\text{--}2.1\mu\text{m}$ (Stage 5); $0.65\text{--}1.1\mu\text{m}$ (Stage 6); $0.43\text{--}0.65\mu\text{m}$ (Stage 7). The flow rate was 28.3 L min^{-1} . Aerosols were collected onto $0.2\mu\text{m}$ pore polycarbonate filters (47 mm; Merck Millipore Ltd., Cork, Ireland).

In each round of sample preparation, two sets of Andersen samplers (named Set A and Set B) and one holder were utilized parallelly and simultaneously in open air (Figure S2-1(a)). Set A was used to measure the bacterial aerosols concentrations originally collected on the stages (i.e., without suspension), and Set B was used to collect filters for suspension (i.e., with suspension). The holder sample (47 mm, Millipore Corp., Billerica, MA, US) with polycarbonate filters was used as the control of total bacterial cell concentration for the Andersen samples. The filters for suspension were sealed in Petri dishes and stored at -20°C until analysis. For suspension process, each collected filter on the Stages 0-6 of Set B was placed in a clean hood for one hour until it returns to the room temperature. The filter in Set B was then reset into the Andersen sampler at the homologous stage of the filter collection in the clean hood with subsequent stages mounted with new filters and upper stages without filters (Figure.S2-1(b)). The sampler was run in the clean hood for a certain time under room temperature ($20\text{--}24^{\circ}\text{C}$) and relative humidity (40-60%).

After that, the filters were used for bacterial enumeration. After suspension, the concentration of each in Set B was shown by the following symbols: N_{BR-n} is the number of bacterial cells in Stage n remained after suspension, which reflects the remained possibilities of bacterial aerosol for the calculation of dropping rates. N_{BP-n} is the sum of the bacterial cells in Stage n remained after suspension and dropping to subsequent stages in Set B, which reflects the concentration without suspension, and parallelly with Set A. N_{BS-n} is the sum of the bacterial cells remained after suspension and receiving from upper stages in Set B, which refers to the bacterial aerosol concentration after suspension, showing the re-distribution.

Before the collection of each sample set, all stages of the sampler were cleaned carefully, and the plates for the filters were rinsed and wiped with 70% ethanol in a clean hood to avoid contamination. A blank control for each set of samples was prepared; i.e., a blank filter was set in the sampler without sample collection. Filters were stored in Analyslide® petri dishes (7231, Pall corporation, New York, USA) at -20°C in the refrigerator.

2.2.2 The preparation of filters

Aerosols samples in open air were collected on the balcony of Environmental & Symbiotic Science North Building (32.32°N , 129.99°E , about 20 m above ground level) in the campus of the Prefectural University of Kumamoto, southwestern Japan. The campus is in a residential area and few anthropogenic sources of air pollutants around the sampling site. Samples were collected between September of 2019 and March of 2020. More details about sampling time in the open air and suspension were shown in Table S1-1. In each group of suspension experiments, three parallel rounds of samples were prepared. In-line filter holders were applied to collect samples to identify the consistency of the concentration of total bacterial cells measured with Andersen samplers and holders. The flow rate was 19 min/L.

In this study, we prepared 7 groups of samples in different periods. Each group included 3 parallel rounds. In each round, 2 sets samples of Andersen sampler and 1 holder sample were collected. In total, 1050 filter samples were prepared, besides blank filters for quality control. Back up filters were also applied to understand the loss of bacterial aerosol with the air-flow.

In addition, to ensure reliability, the background concentration of the clean hood was also measured with 3 sets of samples collected for 6, 12, and 24 hours, respectively. We found that the concentration in clean hood was always two orders smaller than and less than 10% of the concentration in ambient air. In the development of calibration scheme, the average concentration in clean hood was extracted in the calculation although this extraction had little effect on accuracy.

2.2.3 Identification of bacterial cells

The bacterial cells in the samples were investigated by using the BacLight live/dead staining method (Murata & Zhang, 2013). Bacterial cells and other particles were detached from the aerosols-loaded polycarbonate membranes (47 mm in diameter) in phosphate-buffered saline solution (PBS, pH 7.4) by vortex shaking and ultrasonic vibration in ice bath. Then the suspension was treated with glutaraldehyde fixation and stained with the LIVE/DEAD BacLight Bacterial Viability Kit (L13152, Invitrogen™, Molecular Probes Inc., Eugene, Oregon, US), followed by filtration on a 25 mm diameter and 0.2 μm pore black polycarbonate membrane for bacterial enumeration. The viable and nonviable bacterial cells on the filters were enumerated with an epifluorescence microscope (EFM; Eclipse 80i, Nikon Corp., Tokyo, Japan). An excitation wavelength range between 450 and 490 nm (blue) was utilized, and the microscope was operated at 1000 magnification. Fluorescent green and red/orange/yellow cells with spherical shape and size close to or smaller than 1 μm in diameter were counted as viable and nonviable bacteria, respectively. The cell concentrations in the size-segregated particles in the air were estimated based on cell counts and the sampling of air volumes after the subtraction of their blank control. In this paper, we focus on the sum of viable and nonviable cells for simplification, because we found the majority of bacterial cells were viable ones and they dropped more easily from the filters than nonviable ones.

2.2.4 Dropping rate and transfer coefficient

Using the bacterial counts on the filters of Stage n with and without the suspension, the dropping rate for Stage n , DR_n , is determined with Eq. (1):

$$DR_n(t) = \left(1 - \frac{N_{BR-n}}{N_{A-n}}\right) \times 100\% \quad (1)$$

where N_{A-n} is the bacterial counts of Stage n filter (from Set A) without the suspension, N_{BR-n} is the bacterial counts remained in Stage n filter (from Set B) after the suspension (Figure S2-2(a)), and t is the suspension time. The dropping rate DR_n refers to the transfer possibility of bacterial cells from Stage n to subsequent stages during the suspension time t .

To describe the transfer of bacteria from Stage m to Stage n , a parameter, named transfer coefficient φ_{mn} was introduced (Table S2-2). It refers to the rate of bacterial movement from Stage m to Stage n , and is determined with Eq. (2):

$$\varphi_{mn} = \frac{N_{mn}}{N_{A-m} - N_{BR-m}} \quad (2)$$

where N_{mn} is the bacteria number moving from Stage m to Stage n during the suspension time (Figure S2-2(a)).

2.2.5 Calibration equation

The calibration scheme for each stage is based on the relationship between the dropping rate of bacterial aerosols and suspension time with assumption that dropped bacteria are always trapped by subsequent stages according to the transfer coefficient φ_{mn} .

The possibility of remained bacteria on Stage n after sample collection time t is:

$$f_n(t) = 1 - DR_n(t) \quad (3)$$

The proportion of remaining bacteria can be calculated by integrating $f_n(t)$.

The calibrated bacterial concentration of Stage 0, i.e., the top stage and the size range of $>11 \mu\text{m}$, is calculated with Eq. (4):

$$C_0 \int_0^t f_0(t) dt = t C_0' \quad (4)$$

where C_0 is the concentration of airborne bacterial cells in the size range of Stage 0 after calibration, and C_0' is the original concentration calculated with the bacterial counts on the filter of Stage 0.

For other stages, the movement of bacteria from upper stages should be taken into the consideration, and the concentration could be calculated with Eq. (4):

$$F C_n \int_0^t f_n(t) dt = Ft C_n' - \sum_{m=0}^{n-1} C_m \varphi_{mn} \quad (5)$$

where C_n is the concentration of airborne bacterial cells in the size range of Stage n, C_n' is the concentration calculated with the bacterial counts on the filter of Stage n, C_m is the concentration of airborne bacterial cells in the size range of Stage m which is the upper stage of Stage n, and F is the sampling flow rate.

2.3 Results

2.3.1 Concentration and size distribution with and without the suspension

Table 2-1 Total concentration of bacterial cells ($\times 10^5$ cells $\mu\text{m}^{-1} \text{m}^{-3}$) from Andersen samples Set A, holder samples, and Andersen samples Set B after suspension in the clean hood in three round experiments according to sample collection time (CT in hours) (*suspension time for Set B in hours).

CT	Set A	Holder	Set B	
6	5.1 \pm 0.7	5.6 \pm 0.9	4.9 \pm 0.5	6*
12	4.6 \pm 0.5	5.3 \pm 0.3	4.7 \pm 0.8	12*
24	4.2 \pm 0.8	4.9 \pm 0.6	4.0 \pm 0.5	24*

The total bacterial cell concentration in average measured from Set A (without suspension) was generally consistent (4.6 \pm 0.7 cells $\mu\text{m}^{-1} \text{m}^{-3}$) with that from Set B (after the suspension), and also in good agreement (4.5 \pm 0.6 cells $\mu\text{m}^{-1} \text{m}^{-3}$) with the concentration obtained from holder samples in each round experiment for the investigation of the dropping rates (Table 2-1). In this table, the concentration N_{BP-n} is shown for Set B, which is the sum of the bacterial cells in Stage n remained after suspension and dropping to subsequent stages in Set B, which reflects the concentration without suspension, and parallelly with Set A. The data of each round and an example of N_{BP-n} concentration in Set B were given additionally in Table S2-3 and Table S2-4 in SI. After the suspension, the total concentration of bacterial cells varied no more than 10% in comparison with and without the suspension. Durand et al. (2002) also reported similar result that confidence can be placed on longer-term samples for total microbes collected on filter media by polystyrene cassettes. The consistence indicated the prolonged sampling time did not affect the total concentration of bacterial aerosols by filter-media sampling.

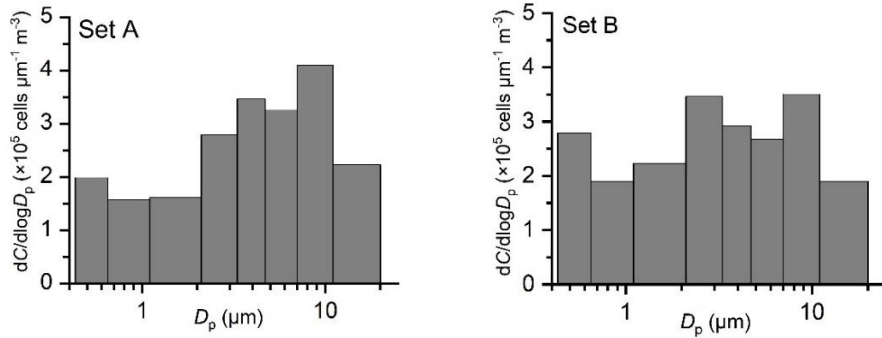


Figure 2-1 Bacterial aerosols size distribution (Diameter D_p) for 6 hours sampling without suspension (a) and with 6 hours suspension (b) in the clean hood.

In most cases, there were obvious changes in the number size distribution of bacteria due to the suspension, and an example is shown in Figure 2-1. In Figure 2-1(b), the concentration of N_{BS-n} is illustrated, which is the sum of the bacterial cells remained after suspension and receiving from upper stages in Set B, indicating the re-distribution. After a suspension for 6 hours, the movement of bacteria from large size ranges to small size ranges were confirmed and the distribution of bacteria according to size ranges changed due to the suspension. The dropping rates differed according to size. Therefore, prolonged sample collection time may cause uncertainties in the measurement of the number size distribution although the movement is expected to have less impact on the concentration of total bacteria.

2.3.2 Variation of dropping rates according to size ranges

Table 2-2 Dropping rate DR_n (%) for samples of Stages 0-6 (μm) according to sample collection time (CT) and the suspension time in the clean hood (ST).

CT	ST	Stage 0	Stage 1	Stage 2	Stage 3	Stage 4	Stage 5	Stage 6
(hrs)	(hrs)	(>11)	(7-11)	(4.7-7)	(3.3-4.7)	(2.1-3.3)	(1.1-2.1)	(0.65-1.1)
6	6	49.1±9.4	53.9±10.3	48.7±8.9	30.8±7.5	26.2±11.3	11.8±9.9	9.5±7.9
12	12	50.1±15.4	45.9±12.2	44.6±14.4	37.9±13.6	29.5±10.6	15.2±7.4	10.2±8.6
24	24	43.2±6.7	51.5±9.5	40.4±11.5	29.6±12.3	28.3±11.4	19.5±17.6	8.5±7.6

Table 2-2 shows the dropping rates of bacterial cells according to size ranges when the suspension time was equal to the collection time for 6 hours, 12 hours, and 24 hours. The dropping rates for different size ranges were similar even though the suspension time differed largely,

suggesting the dropping mainly occurred in the initial periods of the suspension, i.e., the time < 6 hours (Hu et al 2020). However, the dropping rates varied from size to size and bacteria in larger size ranges moved frequently to smaller size ranges. The dropping rates were 40–50% in size ranges of > 4.7 μm , which were significantly higher than those in the size range of 2.1–3.3 μm ($p < 0.01$). In the size range of 2.1–3.3 μm , 30%–40% of the bacteria dropped to subsequent stages, which were significantly higher than 1.1–2.1 μm ($p < 0.01$). The dropping rates of bacterial aerosols 1.1–2.1 μm were 12%–20% depending on suspension time. For size range of 0.65–1.1 μm (Stage 6), there is the only one Stage 7 (0.43–0.65 μm) in the subsequent, and rare fluorescent cell can be found in microscopic field for back-up filters, so Stage 7 (0.43–0.65 μm) was supposed to receive most of the dropping bacteria from upper stages.

The difference of dropping rate with particle size ranges is mainly attributed to the existence of airborne bacterial aggregates consisting of two or three single cells and particles (Hu et al., 2020). Larger aggregates have higher inertia and larger surface area, and are more easily to be trapped on upper stage filters and then disaggregated. According to Xu et al. (2013), impaction stress correlates with size range, and larger bacterial particles tend to sustain higher impaction stress compared to smaller ones. Besides, bioaerosol particles collected by lower stages of Andersen samplers might have been impacted more times before their collection due to particle bounce on the surface of filters. These results indicate that filters in stages of larger size ranges likely tended to lose bacterial cells easier.

2.3.3 Dependence of dropping rates on suspension time

Table 2-3 Dropping rates DR_n (%) for samples of Stages 0 - 3 for different suspension time in the clean hood (ST). The collection time of the samples was 6 hours.

ST (hrs)	Stage 0 (>11 μm)	Stage 1 (7-11 μm)	Stage 2 (4.7-7 μm)	Stage 3 (3.3-4.7 μm)
0.5	5.6±0.1	9.0±2.3	1.5±0.4	8.6±1.3
1.0	14.7±0.1	12.7±6.7	17.6±5.3	6.5±3.3
3.0	28.3±11.2	18.6±8.9	18.5±7.9	18.1±5.1
6.0	42.2±15.4	41.0±12.2	39.3±5.4	30.5±9.6
12.0	50.1±12.4	46.0±10.7	43.6±9.5	37.9±6.7
24.0	49.6±14.0	46.5±17.0	41.1±6.7	36.4±5.4

The dropping rates for Stages 0–3 with different suspension time including those smaller than

6 hours are summarized in Table 2-3. Other stages are not included because the dropping rates from Stage 4 were less than 11.1% and had less influence on the size distribution. The concentration of Stage 4 (2.1-3.3 μm) was 0.59 and 0.65×10^5 cells $\mu\text{m}^{-1} \text{m}^{-3}$ before and after the exponential calibration in this size range (Table S2-4). The uncertainties of subsequent size ranges 1.1-2.1 μm , 0.65-1.1 μm , 0.43-0.65 μm (Stages 5, 6, and 7) were much smaller than Stage 4 (Table 2-2), so the exponential calibration of the subsequent Stages 5, 6, and 7 are not considered.

The dropping rates for all different size ranges were below 10% when the suspension time was 0.5 hour, and the dropping rates were around 20% when the suspension time was less 3 hours. When the suspension time was 6 hours, the dropping rates of bacteria on the filters were 42.2%, 41.0%, 39.3%, and 30.5% for size range $>11 \mu\text{m}$, 7.0-11 μm , 4.7-7.0 μm , and 3.3-4.7 μm (Stages 0, 1, 2, 3 and 4), respectively. The dropping rates increased largely with time when the suspension time was within 6 hours. When suspension time was over 6 hours, the dropping rates for each stage tended to be stable as described above. The dropping rates for different stages when the suspension time was 12 and 24 hours were similar and only slightly larger than that for 6-hour suspension time. In summary, more bacterial cells or aggregates dropped to lower stages within the first 6 hours with suspension time increased, and the extension of suspension time enlarged uncertainties in larger size ranges. That means bacteria trapped in filters on upper stages easily dropped to lower stages in early time.

Fig. 2-2 shows the variation in dropping rates of bacteria according to suspension time for size ranges of $>11 \mu\text{m}$, 7.0-11 μm , 4.7-7.0 μm , 3.3-4.7 μm (Stages 0-3). The best statistical regression relations between the dropping rate from the stages and the suspension time were exponential functions in the form of $DR_n(t) = \alpha + \beta e^{\mu t}$ with constants α , β and μ . The correlation coefficients of the regression functions were significantly high ($R^2 \geq 0.96$), reflecting the high confidence of the exponential functions (Figure 2-2, Table S2-3).

With the exponential functional relationship between the dropping rate and the suspension time, the correspondent dropping rates of a filter used with the Andersen samplers according to sample collection time can be obtained. Then the actual number size distribution of the bacterial aerosols in the air is able to be acquired with Eq. (3) and Eq. (4) from the distribution measured with the Andersen samplers (Text 1 in Supplementary).

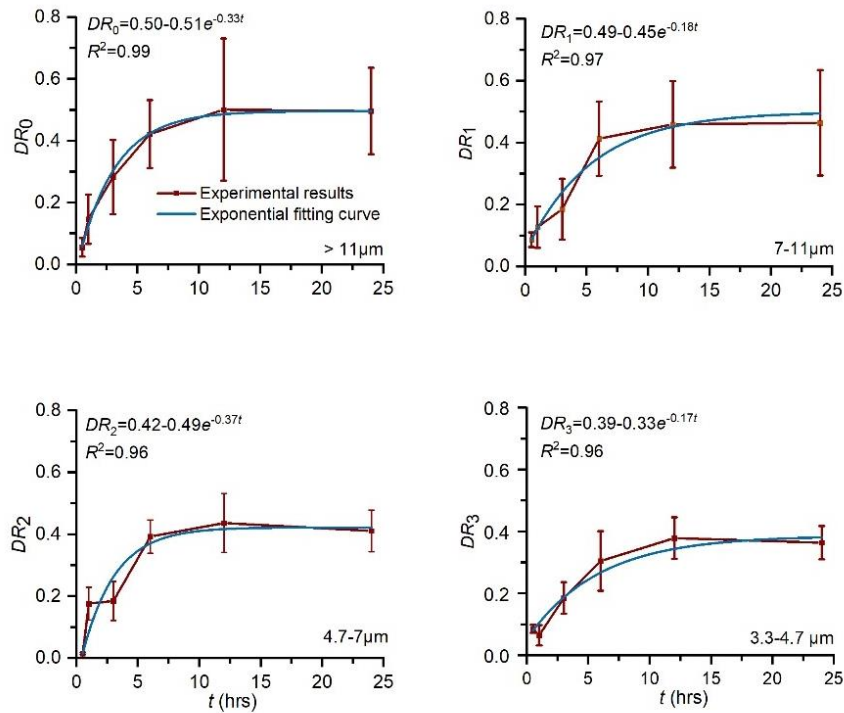


Figure 2-2 Variation of dropping rate of bacterial aerosols in size ranges of $>11 \mu\text{m}$ (Stage 0), and $7.0\text{--}11 \mu\text{m}$ (Stage 1), $4.7\text{--}7.0 \mu\text{m}$ (Stage 2), and $3.3\text{--}4.7 \mu\text{m}$ (Stage 3) with the suspension time, and exponential fitting curves. The points in this figure represent the average experimental values with standard deviations marked with the vertical error bars.

According to the calibration schemes, the uncertainties due to the movement of bacteria from upper stages to lower stages during the sample collection need to be calibrated when the collection time is longer than a certain time. For Andersen samplers used in the present study, the sample collection time leading to 10% uncertainties was 0.32 hour for Stage 0 ($>11 \mu\text{m}$), 0.35 hour for Stage 1 ($7.0\text{--}11 \mu\text{m}$), 0.50 hour for Stage 2 ($4.7\text{--}7.0 \mu\text{m}$) and 0.33 hour for Stage 3 ($3.3\text{--}4.7 \mu\text{m}$). The collection time for the 4 stages is less than 0.70, 1.06, 0.94 and 1.41 hour, respectively if the dropping rate is below 20%. Therefore, the sample collection time in order to suppress the uncertainties less than 10% should be less than about 20 minutes, and should be less than about 40 minutes to suppress the uncertainties less than 20%.

2.4 Application examples

As application examples of the calibration scheme, the results of three ambient cases of Andersen samples with sample collection time of 2, 5, and 16 hours before and after the calibration are given in Figure 2-3 and Table S2-4.

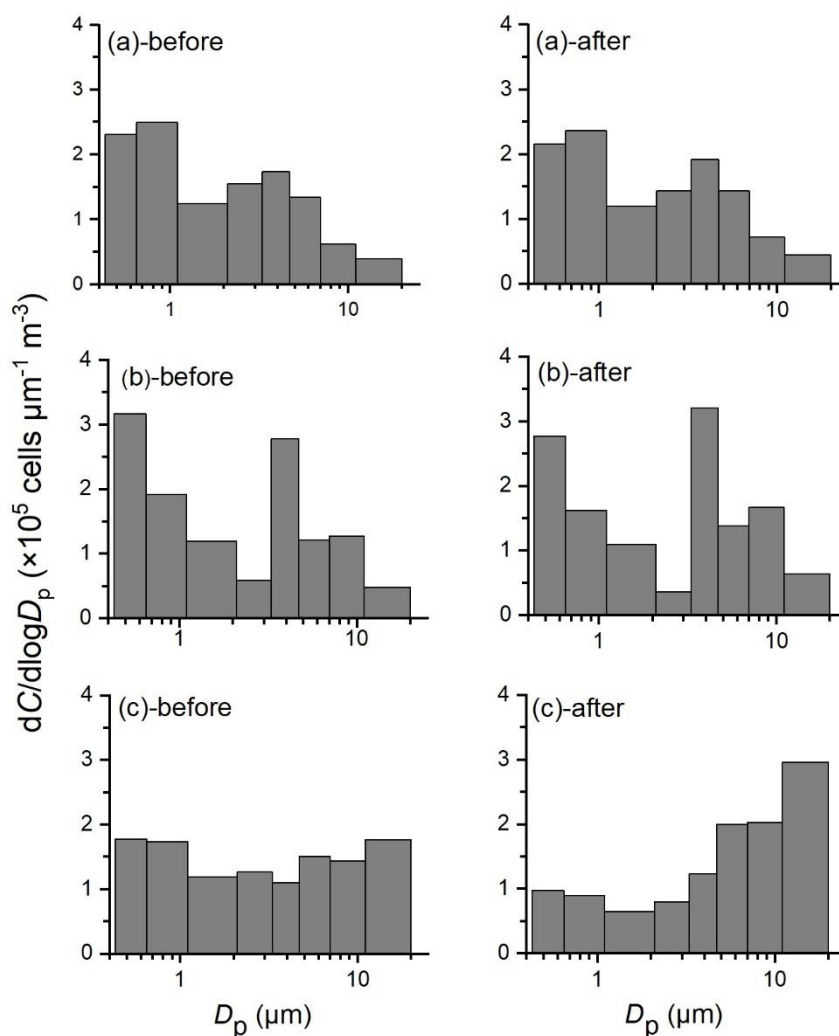


Figure 2-3 Number size distribution of bacteria from three sets of Andersen samples before (left) and after (right) the calibration. The samples were collected on the platform of a building in southwestern Japan (32.324° N , 129.993° E) on March 25-27, 2018. The sample collection time was 2 hours for (a), 5 hours for (b), and 16 hours for (c).

When the sample collection time was 2 hours, the distributions before and after the calibration were similar. The highest concentration was 2.5×10^5 cells $\mu\text{m}^{-1} \text{m}^{-3}$ in the range of 0.65-1.1 μm (Stage 6), and it decreased by 5.0% and became 2.4×10^5 cells $\mu\text{m}^{-1} \text{m}^{-3}$ after the calibration (Figure 2-3a). The biggest difference was in the range of $> 11 \mu\text{m}$ (Stage 0), and the concentration increased from 0.38×10^5 cells $\mu\text{m}^{-1} \text{m}^{-3}$ to 0.44×10^5 cells $\mu\text{m}^{-1} \text{m}^{-3}$. The increase or decrease rate due to the calibration was under 15% for all size ranges.

For the case of 5 hours samples (Fig. 3b), the number size distribution before the calibration was bimodal with the pick modes around 0.43-0.65 μm (Stage 7) and 3.3-4.7 μm (Stage 3). The calibration did not lead to large variation to the distribution, except some details. Before the calibration, the peak concentration appeared at Stage 7 and was 3.2×10^5 cells $\mu\text{m}^{-1} \text{m}^{-3}$. After the calibration, the concentration was 2.7×10^5 cells $\mu\text{m}^{-1} \text{m}^{-3}$, 14.6% smaller than that before the calibration. The peak in range of 3.3-4.7 μm (Stage 3) increased by 18.2% to 3.3×10^5 cells $\mu\text{m}^{-1} \text{m}^{-3}$. The biggest change happened in size range of 2.1-3.3 μm (Stage 4) and the concentration decreased by 51.4% after the calibration, but it did not influence the distribution considerably because of the low concentration.

For the case of 16 hours samples (Fig. 3c), the distribution before and after calibration was apparently different. Before the calibration, the concentration in all size ranges varied in a narrow range between 1.1×10^5 cells $\mu\text{m}^{-1} \text{m}^{-3}$ (Stage 3: 3.3-4.7 μm) and 1.8×10^5 cells $\mu\text{m}^{-1} \text{m}^{-3}$ (Stage 7: 0.43-0.65 μm). The distribution did not have an apparent mode. After the calibration, the distribution had a clear mode in larger size range. The peak appeared in the range of $> 11 \mu\text{m}$ (Stage 0: calculated with 11–20 μm) and the concentration became 3.0×10^5 cells $\mu\text{m}^{-1} \text{m}^{-3}$, which increased by 67.7% in comparison with before the calibration.

2.5 Discussion

This study is the first attempt to reduce possible uncertainties in measuring the number size distribution of airborne bacteria with Andersen samplers. Upon the present results, the number size distribution of airborne bacteria measured directly from a size-segregated sampler might have large uncertainties when the sample collection time was longer than a certain time. The most effective way to suppress the uncertainty is to shorten sample collection time. However, sample collection time could not be very short because it is necessary to collect adequate amount of bacterial cells on a filter in order to ensure the confidence of bacterial cell counting from the filter. The time is dependent on the bacterial concentration in the air, the flow rate of sample collection,

and the sensitivity of the methods used to enumerate bacterial cells in the samples. For the BacLight live/dead staining method we used, the smallest volume of sample collection air for confident bacteria counting is 0.25 m^3 when the bacterial concentration is around $10^5 \text{ cells m}^{-3}$ (Hara et al., 2011; Murata and Zhang, 2013). Regarding the flow rate of the Andersen samplers we used in this study was 28.3 L min^{-1} , the shortest collection time for a set of samples of the eight stages should be about one hour assuming that airborne bacterial cells trapped in all filters are in same orders. If the concentration of bacteria in the air is higher, for instance under dust conditions, the sample collection time could be shortened. Otherwise, the collection time need to be extended to ensure more accurate results, for which the calibration is inevitable in order to limit the uncertainties in the results on number size distribution of airborne bacteria less than 10%.

One concern we did not investigate but may largely influence the results is the filter type used in the sample collection. Polycarbonate filters (47 mm; Merck Millipore Ltd., Cork, Ireland), a type of filters frequently adopted in aerosol particles studies, were used in the preparation and application tests in the present study. It is supposed that the dropping of bacterial cells from the filter could be influenced, sometimes largely, by the structure of the filter surface. There are other frequently-used types of filters, such as Teflon filters, quartz fiber filters, and glass fiber filters, etc. The surface structure of these filters is very different from that of polycarbonate filters. For example, fiber filters may trap particles more tightly than polycarbonate filters because the surface of fiber filters is nets of fibers while that of polycarbonate filters is plain and smooth. The dropping rate of bacteria for polycarbonate filters should be larger than that for fiber filters. The calibration scheme has to be reconstructed in cases when other types of filters are adopted even for the same type of samplers. That means for each type of Andersen sampler and each type of filters used for sample collection, a calibration scheme needs to be constructed.

The dropping rates reflect that the uncertainties could be relative to a load of bioaerosols in the air, temperature, humidity, wind, etc. The sample collection for the suspension test was actually a process of accumulation and dropping, which was not considered in this study. The influence of this simplification on the results is expected small because the measured concentration represented the average and could be considered the concentration during the sample collection periods. In addition, easily dropping bacteria might have dropped from filters in the preparation process, leading to an underestimate of the dropping rates. That means the uncertainties in the present assessment might have been underestimated and better methods to prepare the filter for the establishment of calibration scheme are necessary.

2.6 Summary

Dropping of bacterial cells from upper stages to lower stages of Andersen samplers during impaction was investigated in order to quantify the uncertainties in number size distribution of airborne bacteria measured by using traditional size-segregated aerosol samplers. Suspension experiments were conducted in clean hood and the correlation between the uncertainties and sampling time for each available size range was obtained. Based on the results, a calibration scheme was proposed to reduce the uncertainties in the distribution measured with the Andersen samplers in this study. We confirmed that bacterial aerosols in larger size ranges moved to smaller size ranges during the impaction of the samplers, resulting uncertainties in different size ranges. Significant exponential correlations were obtained between the suspension time and calibrated dropping rates. In the present study, the sampling time should be within 20 minutes or 40 minutes in order to suppress the dropping rate below 10% or 20%, respectively. In case sampling time is longer than mentioned, calibration is strongly recommended. With the calibration scheme we developed, we confirmed the large shift of mode size range in the number size distribution of airborne bacteria after the calibration in some cases.

The number size distribution of bioaerosols, including bacteria, virus, fungi, etc., is the basis for the assessment of their dissemination in the air from local scale to global scale, their deposition potentials to different parts of respiratory organs, and their activations in cloud and ice cloud formation. The present results suggest that sample collection time should not be extended without considering the dropping of bioaerosols during sample collection and it is necessary to carefully consider the calibration in case of long-term sample collection with traditional size-segregated samplers. This study provides an example way to approach the dropping problem during sample collection. Future studies on the calibration could avoid the uncertainties in filter preparation by chambers or ASHRAE wind tunnels to implement a better calibration approach.

Chapter 3

Number size distribution of bacterial aerosols in terrestrial and marine airflows at a coastal site of southwestern Japan

3.1 Introduction

In terms of variations in size distribution of bacterial aerosols in the atmosphere, several studies have been conducted to investigate their influencing factors. For example, unimodal patterns were attained for total airborne microorganisms with a peak of 2.1–3.3 μm in Xi'an, western China during hazy episodes (Yang et al., 2021), whereas a bimodal size distribution of airborne bacteria was observed with two peaks, 1.1–2.1 μm , and 4.7–7.0 μm in Qingdao, eastern China (Yin et al., 2021). Therefore, bacterial aerosols in a specific area vary substantially according to their origin and source location.

It has been reported strong variation in size distribution of airborne microorganisms, probably due to the seasonal changes in air masses (Yin et al., 2021), indicating the spread of airborne particles with airflow may closely depend on the particle size. However, the size-differential concentration of bioaerosols has not been systematically measured because of difficulties in sample collection and quantification. In particular, the differences in bioaerosol size distribution according to airflow have not been carefully investigated, leaving variations unknown in bioaerosols according to size and weather. In this chapter, we report the results of our observations of the number size distribution of bacterial aerosols under different synoptic weather conditions at a coastal site in southwestern Japan, using the eight-stage Andersen sampler and calibrated by the scheme in Chapter 1. The purposes of this chapter are: 1) to quantify the number size distributions, investigate their variation according to weather conditions; 2) to explore the size-dependent characteristics of the dispersion and activities of bioaerosols on local, regional, and large scales; 3) to understand the bacterial removal in dry deposition by estimation.

3.2 Materials and methods

3.2.1 Sample collection

Number size distribution of bacterial aerosols was observed at a coastal site in Amakusa, Kumamoto, southwestern Japan (32.324°N, 129.993°E, 23 m a.m.s.l) during several observational campaigns in the spring of 2014, 2015, 2017, and 2018. This site is located on the seaside with the sea areas in the south and the west, and with the island areas in the north and east. From the end of October to the beginning of next May, this site is usually under the influence of the Northern Hemisphere mid-latitude westerlies, and the wind frequently comes from the Asian continent and the Yellow Sea areas between China and Japan. From mid-May to October, local

sea/land breezes and airflow from the marine areas in the south or southeast (East China Sea and Pacific) prevail. In addition, the influence of anthropogenic air pollutants from local areas is minimal. The sample collection was started and stopped according to the variation of weather to ensure that each sample was collected in a period under similar weather conditions. There are only a few fisheries and agricultural activities in areas close to the site and sporadic small farms several kilometers away from the site in the north, resulting in a minimal background concentration in the local area rendering the site suitable for the observation of airborne aerosols originating from distant areas reaching the site via long-distance transport.

Aerosol particles were collected onto 0.2 μm pore polycarbonate filters (47 mm; Merck Millipore Ltd., Cork, Ireland) using eight-stage Andersen samplers (Model AN-200; Tokyo Dylec Corp., Japan) at a flow rate of 28.3 L min^{-1} . The particles were size-differentially trapped onto filters in eight aerodynamic diameter ranges: >11, 7.0–11, 4.7–7.0, 3.3–4.7, 2.1–3.3, 1.1–2.1, 0.65–1.1, and 0.43–0.65 μm . It has been proved that dust particles were mainly in the size range of larger than 1 μm when Asian dust appeared in Japan (Fan et al., 1996; Okada and Kai, 2004; Zhang et al., 2000). For this reason, 1 μm was used as the critical value to separate the fine and coarse aerosols in the present study. For each set of size-segregated samples, two in-line holder samples were collected using the same type of filter. The concentration of bacterial cells from the holder samples was compared with the combined concentration of the entire size range of the Andersen samplers to ensure the confidence of sample collection.

3.2.2 Backward trajectories and meteorological conditions

The backward trajectories of air parcels from the samples collection points were calculated using the National Oceanic and Atmosphere Administration Hybrid Single Particle Lagrangian Integrated Trajectory model (<https://www.ready.noaa.gov/HYSPLIT.php>) to investigate the potential sources of the particles according to the movement of mass towards the sampling site. The calculation incorporated the time from the beginning to the end of each sample collection period. For each sample, the backward trajectories were measured for 72 h at starting altitudes of 500 m, 1000 m, and 1500 m above ground level at the observation site. The transported distance was attained by the Haversine formula based on the longitudes and latitudes on the air parcels' trajectories with one-hour resolution.

An air parcel can remain in a close to adiabatic state, and the influence of emissions from local areas is usually low if it moves quickly. In contrast, if the movement of air is slow or stagnant, it is usually highly influenced by emissions from local areas. Therefore, to investigate the moving speed of the air parcel around the sampling site, the distance of the air parcels in the preceding 72

h was estimated from the back trajectories.

Meteorological conditions, including temperature, surface pressure, relative humidity, wind speed, wind direction, and precipitation, were monitored at the observation site. In addition, weather charts and conditions issued by the Japan Meteorological Agency (<https://www.jma.go.jp/>) were used as references.

3.2.3 Categories of samples in terms of potential sources

Samples were categorized into five groups according to the meteorological conditions and backward trajectories of the air parcels from which the samples were collected. The classification was based on weather charts (<http://www.data.jma.go.jp/fcd/yocho/hibiten/index.html>), variations in surface pressure (Fig.S1-1), and backward trajectories (Fig.S2-2). The LDT group represents the samples mainly dominated by long-distance transport of air via western and northwestern winds; that is, the samples were primarily affected by terrestrial source air masses from the Asian continent. Weather conditions showed that the LDT samples were collected in the postfrontal air of cyclones when the surface pressure gradually decreased and the weather became unstable. The LDM group represents the long-distance transport of marine air and usually originates from the south and prefrontal regions of cyclones. These samples were primarily affected by marine air masses. Fig. 1 shows the backward trajectories of the air parcels for the LDT and LDM groups. The LSL and LSS groups comprise samples collected in the land breeze and sea breeze, respectively; when the weather is stable and dominated by anticyclones, the wind is weak, and the air movement is stagnant. The MIX group samples were collected when the anticyclones approached the site after the passage of the cyclones. The weather was characterized by weak winds and a gradual increase in surface pressure, and the air parcels moved slowly from the direction of the Asian continent. The MIX samples contained long-distance transported aerosols from the mainland and many locally emitted aerosols because of the slow movement of the air. More information on the sample collection is shown in Table 3-1. For LDT1, Asian dust was reported by the Japanese Meteorological Agency and confirmed during sample collection (https://www.data.jma.go.jp/gmd/env/kosahp/kosa_map_20150322.html). The occurrence of Asian dust in observation areas usually coincides with high concentrations of airborne bacterial cells (e.g., Hara and Zhang, 2012; Hu et al., 2020). Asian dust was not reported for LDT2–LDT5, although the air parcels traveled quickly to the observation areas from the Asian continent via westerly winds.

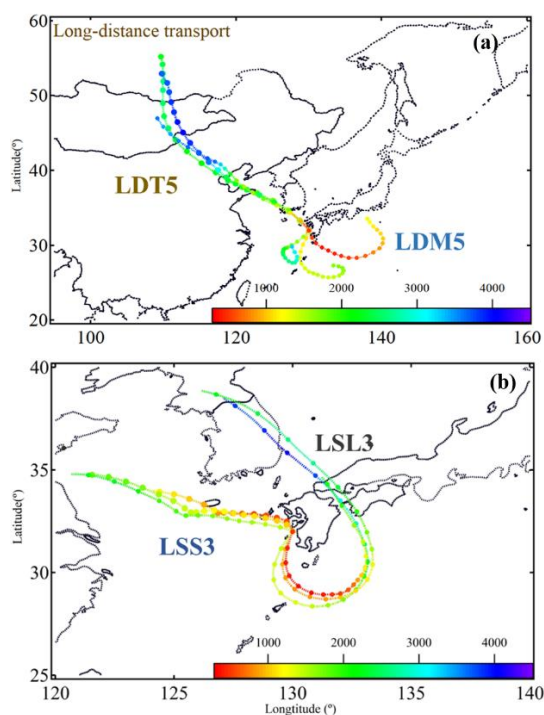


Figure 3-1 Location of the sampling site. Examples of 72-hour backward trajectories are shown in the map for samples in (a) long-distance transported air and (b) local breeze air. LDT represents the sample of long-distance transported terrestrial air, LDM represents the sample of long-distance transported marine air, LSL represents the sample of local scale land breeze, and LSS represents the sample of local scale land breeze. Numbers in the abbreviations stand for the numbered sample cases. Markers on the trajectories stand for 4-hour intervals and colors show the moving height of the air parcels.

Table 3-1 Sample collection time and air mass characteristics. (LDT: Long-distance transport from terrestrial source; LDM: Long-distance transport from marine source; LSL: Local scale land breeze; LSS: Local scale sea breeze; Mixed: mixed with long-distance transport and local breeze)

Group	Date	Sample ID	Start-Stop time	Duration	Synoptic weather
LDT (n=5)	2015022	LDT1*	23:28-5:00	5h32min	Postfront air
	20170521	LDT2	9:00-15:00	6h	
	20150325	LDT3	8:02-8:02	24h	
	20150324	LDT4	8:03-8:02	23h59min	
	20170521	LDT5	1:11-6:00	4h39min	

LDM (n=5)	20170520	LDM1	0:31-3:23	2h52min	Prefront air
	20180328	LDM2	0:28-6:00	5h32min	
	20180328	LDM3	9:00-15:00	6h	
	20180327	LDM4	20:12-00:10	3h58min	
	20180512	LDM5	18:00-23:00	5h	
LSL (n=6)	20140322	LSL1	22:00-12:10	14h10min	Anticyclone air
	20140323	LSL2	12:40-12:40	24h	
	20140324	LSL3	12:40-12:30	23h50min	
	20140328	LSL4	12:30-19:45	7h15min	
	20170519	LSL5	9:00-15:00	6h	
	20180326	LSL6	18:00-23:00	5h	
LSS (n=5)	20180325	LSS1	9:02-15:00	5h58min	Anticyclone air
	20180325	LSS2	17:00-23:00	6h	
	20180326	LSS3	01:00-06:00	5h	
	20180327	LSS4	00:00-06:00	6h	
	20170518	LSS5	9:11-15:00	5h49min	
MIX (n=4)	20150326	MIX1	6:03-6:50	24h47min	Approaching anticyclone air
	20170324	MIX2	9:35-18:00	8h25min	
	20170325	MIX3	10:30-12:38	2h8min	
	20170325	MIX4	14:30-17:30	5h	

* Asian dust was reported by the Japanese Meteorological Agency.

3.2.4 Enumeration and calibration

The bacterial aerosols in the samples were identified using BacLight staining. A phosphate-buffered saline solution removed bacterial cells and other particles from the filters by vortexing and ultrasonic vibration in an ice bath. The suspension liquid was then fixed with glutaraldehyde on black filters (25 mm, black polycarbonate filter, Advantec®, Toyo Toshi Kaisha, Ltd., Japan) and stained with LIVE/DEAD BacLight Bacterial Viability kits. The kits stained viable bacterial cells green and non-viable bacterial cells red under epifluorescence microscopy (Murata and Zhang, 2013). After staining, the bacterial cells in the filter sample were enumerated under an epifluorescence microscope from 20 random fields of 100 $\mu\text{m} \times 100 \mu\text{m}$. When viewed under a microscope, green or red spherical spots with a size close to or smaller than 1 μm in diameter were considered

bacteria (Hara and Zhang, 2012). However, the presence of cells on filters in the size range exceeding 1.1 μm does not mean that the size of those cells was larger than 1.1 μm . Therefore, the cells were considered to be combined with particles larger than 1.1 μm and were trapped on the relevant filters based on the size segregation of the particle agglomerations (Hu et al., 2020).

The filter samples collected with in-line holders were treated and analyzed the same way as those of the size-segregated samples. The total cell count from the filter was compared to the integrated cell counts of the relevant size-segregated filter samples. If the two counts were similar, the cell numbers in different size ranges from the size-segregated filters were considered acceptable. Otherwise, the results from size-segregated filters were excluded.

After enumeration, the number of bacterial cells in each size range was quantified. Uncertainties were present in the counting of raw data due to the dropping of bacterial cells trapped in the upper-stage filters to lower-stage filters in the samplers during sample collection; therefore, calibration was essential to obtain accurate bacterial cell counts for each size range. Fan et al. (2022) carefully assessed the dropping and uncertainties for the same types of samplers and developed a calibration scheme—this calibration scheme was used in this study. The calibration scheme is suitable only for the total number of cells, that is, the sum of viable and non-viable cells on each size-range filter and calibration schemes have not been established for the separate consideration of viable and non-viable cells. In the following sections, we do not separate viable and non-viable bacterial cells; instead, we focus on the total cell concentration in each size range.

3.2.5 Dry deposition estimation

To investigate the settling potential of bacterial cells in different size ranges and their relative contributions to the total deposition, we estimated the size-dependent dry deposition flux of bacterial cells in each size range using the Sehmel-Hodgson deposition velocity model (Sehmel, 1973). The flux in each size range was obtained using Eq. 1.

$$F_i = C_i \cdot V_{di} \quad (1)$$

where F_i is the dry deposition flux of bacterial cells in the i^{th} size range, C_i is the

concentration of bacterial cells in the same size range, and V_{di} is the dry deposition velocity of bacterial aerosols in the i^{th} size range, which was calculated with a particle density equal to 1.0 g cm^{-3} and the center value of the size range as the diameter of the particles. The dry deposition flux of bacterial cells F_d in the range from the n^{th} to m^{th} range was then obtained using Eq. 2.

$$F_d = \sum_{i=n}^m C_i \cdot V_{di} \quad (2)$$

where the total dry deposition flux is obtained from $n = 1$ to $m = 8$. The results of the fluxes are summarized in three size ranges: fine (0.43–1.1 μm), coarse (1.1–7 μm), and ultra-coarse ($>7 \mu\text{m}$), to investigate their relative importance in the bacterial depositions.

3.3 Results

3.3.1 Distribution in the long-distance transported terrestrial and marine air

The number size distribution of bacterial aerosols in long-distance transport air is shown in Figure 2-2. The results of all sampling periods are depicted in Table S2-2 and Table S2-3 in the Supplement. On average, the concentration of the total airborne bacteria in the LDT group was approximately $9.4 \pm 3.3 \times 10^4 \text{ cells m}^{-3}$, and that in the LDM group was approximately $5.2 \pm 2.8 \times 10^4 \text{ cells m}^{-3}$. The concentration in the LDT cases was 1.8 times that in the LDM cases, indicating a much higher abundance of bacteria in long-distance transported continental air than in long-distance transported marine air. This result is consistent with the fact that microbial cells are much more abundant in continental air than marine air (Hu et al., 2020). The concentration in each size range exhibited distinct differences between the LDT and LDM groups. In the LDT group, the airborne bacteria had a monomodal size distribution with a peak mode at 3.3 – 4.7 μm . The average concentration of the peak mode was $1.1 \times 10^5 \text{ cells m}^{-3} \mu\text{m}^{-1}$, and bacterial cells in the mode size range accounted for 18.7% of the bacterial aerosols over the entire size range. In contrast, the concentration of LDM cases in each size range was small and even, and the number size distribution did not show an obvious peak mode except for an ambiguous peak at 7.0–10.0 μm in some cases. The concentration of each size range fluctuated from $0.2\text{--}0.4 \times 10^5 \text{ cells m}^{-3} \mu\text{m}^{-1}$, making up 10%–16.0% of the bacterial aerosols in the entire size range in the LDM cases. The average concentration in the 3.3–4.7 μm size range in the LDT cases was approximately 4.6 times more than that in the LDM cases, further indicating the difference in the abundance of bacterial

cells in coarse aerosol particle size ranges in terrestrial air.

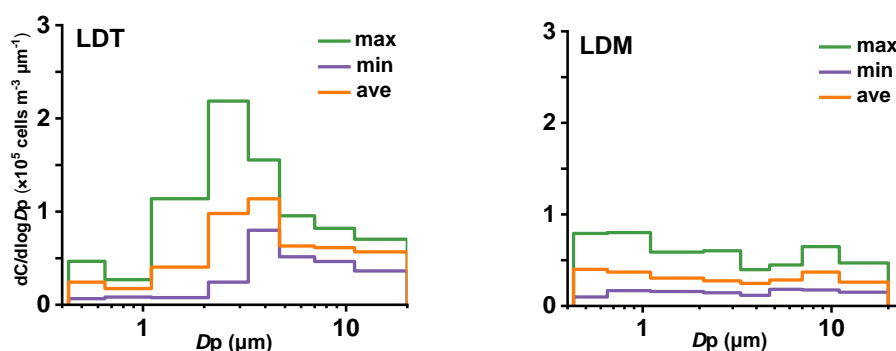


Figure 3-2 Maximum, minimum, and average concentrations of bacterial cells in the eight size ranges for LDT (long-distance transported terrestrial air) and LDM (long-distance transported marine air) groups. Number size distribution of each sample in the LDT and LDM group is shown in Fig.S3 (a) and (b).

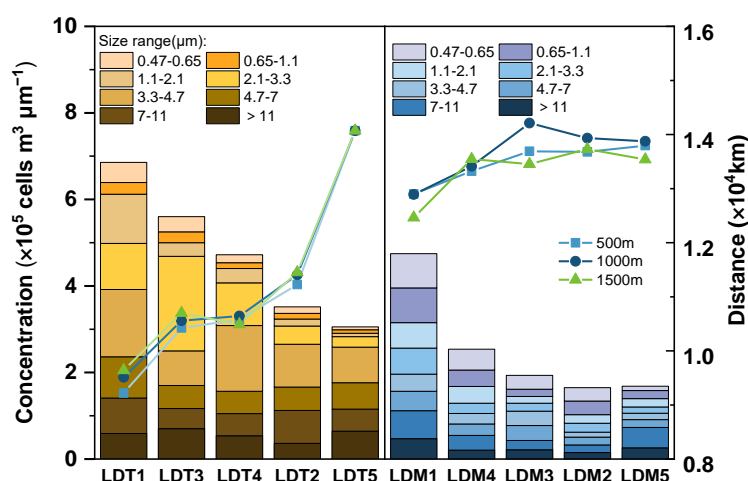


Figure 3-3 Size-differential concentration of bacterial cells versus 72-hour distance of air parcels at the height of 500 m, 1000 m, and 1500 m carrying the bacteria in LDT (long-distance transported terrestrial air) and LDM (long-distance transported marine air) cases.

The correlation between the bacterial aerosol concentration in the different size ranges and the distance of air parcels carrying bacterial cells was investigated to identify the dependence of the size-differential concentration on air parcel movement. Figure 3-2 shows the variation in bacterial aerosol concentration in eight size ranges and the distance of the air parcels in the

preceding 72 h. The correlation between the concentration and the distance is given in Table S3-1.

An obvious phenomenon was that the bacterial concentration decreased proportionally with distance in both the LDT and LDM cases. This result indicates that the faster the air parcel moved in the preceding 72 h, the lower the concentration in the parcel. A previous study on the transport of bacteria in marine air reported similar results to the present LDM cases, in which the concentration of bacteria decreased with an increase in the distance of air parcel movement over the ocean (Mayol et al., 2017).

Figure 3-3 shows that the most significant correlation in the LDT cases was observed in the bacterial aerosol size range of 2.1–4.7 μm and the distances of air masses at an altitude of 1500 m. In the LDM cases, the most significant correlations ($R \geq 0.92$, $P < 0.05$) were observed between the concentration size ranges of $< 3.3 \mu\text{m}$ and distances with the ending point at 500 m. These results suggest that the long-distance transport of bacterial aerosols by westerly winds from the Asian continent was likely dominated by the air mass in an elevated layer, on which the influences from the local areas should be small. In contrast, transport from the sea was more likely due to the transport of air near the sea surface layers on which the influences from the local areas should be prominent.

3.3.2 Distribution in the local land and sea breeze air

The number size distribution of bacterial aerosols showed different patterns and levels in the LSL and LSS cases (Figure 3-4). In other words, the distribution and abundance of bacterial cells differed considerably between the land and sea breezes. On average, the concentration of total airborne bacteria in the LSL group was $1.9 \pm 1.3 \times 10^5 \text{ cells m}^{-3}$, which was approximately four times higher than that of the LSS group at $0.5 \pm 0.2 \times 10^5 \text{ cells m}^{-3}$. The median diameters of bacterial aerosols in the land and sea breezes were 4.01 and 4.31 μm , respectively. The number size distribution was bimodal, with the first peak at 0.43–0.65 μm and the secondary peak at 3.3–4.7 μm in the LSL cases. The average concentration in the first peak size range was $4.0 \times 10^5 \text{ cells m}^{-3} \mu\text{m}^{-1}$, and the bacteria in this peak size range comprised 42.6% of the total bacterial cells in the entire size range. The lowest concentration, $0.4 \times 10^5 \text{ cells m}^{-3} \mu\text{m}^{-1}$, appeared in size range $> 11 \mu\text{m}$, which was approximately one-tenth of the first peak concentration. These results indicate that a local land breeze favors bacterial aerosol accumulation in small-size ranges. In the

LSS cases, the number size distributions did not show clear peak mode size ranges, either coarse or fine. Bacterial cells in each size range accounted for 11.0% to 15.1% of the cells in the entire size range. The results for the LSS cases are similar to those of the LDM cases.

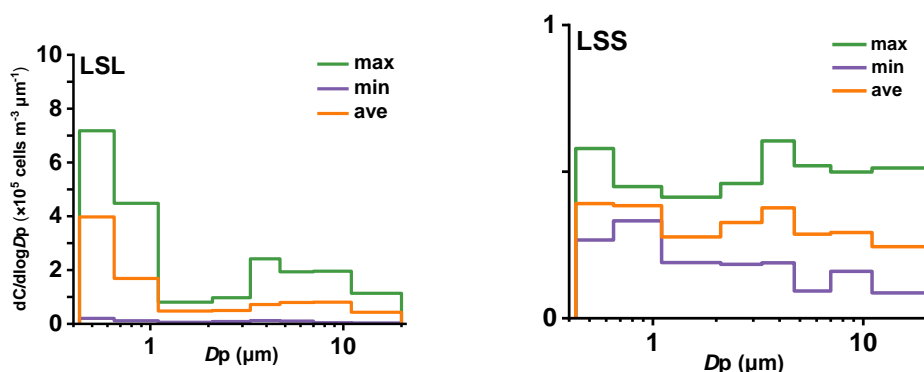


Figure 3-4 Maximum, minimum, and average bacterial cell concentrations in LSL (local-scale land breeze) and LSS (local-scale sea breeze) groups in the eight size ranges. Number size distribution of each sample in the LSL and LSS is shown in Fig.S3 (c) and (d).

Spearman's correlation was conducted to investigate the relationship between the concentration of bacterial cells and local weather conditions (Table 3-2). Wind speed was positively correlated with the concentration of bacterial aerosols in the coarse size range ($R=0.33$, $P<0.01$), mainly distributed in the 3.3–4.7 μm size range ($R=0.32$, $P<0.05$). The concentration showed a significant negative correlation with temperature for both fine and coarse size ranges. Although the correlations were very weak, the results help understand the local weather impact on the concentration of bacterial aerosols. These results were consistent with the sample group categorization because the weather conditions for each group sample had distinctive characteristics. The land breeze was relatively cold and dry with higher wind speed (e.g., LSL1), and sea breeze was relatively warm and moisture with typically lower wind speed (e.g., LSS4), as shown in Table S3-2.

Table 3-2 Spearman's correlation coefficients of the concentration of bacterial aerosols in local land/sea breeze in different size ranges (μm) with the surface weather conditions of temperature (T), relative humidity (RH), wind speed (WS), and pressure (P)

Size Range	T	RH	WS	P
>11	-0.225	-0.039	0.239	0.072
7-11	-0.307*	-0.055	0.303	0.073
4.7-7	-0.298*	-0.120	0.252	0.024
3.3-4.7	-0.385**	-0.129	0.323*	0.173
2.1-3.3	-0.185	-0.090	0.287	0.174
1.1-2.1	-0.261	0.235	0.164	-0.006
0.65-1.1	-0.388**	0.234	0.252	0.072
0.47-0.65	-0.359*	-0.070	0.271	0.324*
Fine (<1.1)	-0.366*	-0.022	0.325	0.220
Coarse (1.1-7)	-0.375*	-0.141	0.325*	0.160
Ultra-coarse(>7)	-0.245	-0.054	0.106	0.217
Total	-0.360*	-0.111	0.309*	0.204

(** $P < 0.01$; * $P < 0.05$)

3.3.3 Distribution in mixed air

Figure 3-5 shows the maximum, minimum, and average bacterial concentrations for the MIX cases. On average, the total concentration of bacterial aerosols was $1.4 \pm 0.8 \times 10^5 \text{ cells m}^{-3}$. This value was higher than the average bacterial aerosol concentration in the LSL group and lower than that in the LDT group. Distinct from the distribution modes of the other categories, the bacterial aerosols were bimodal with two peaks, which was consistent with the influence of long-distance transported air from the Asian continent and the local land breeze. The two peaks were in the size ranges of 0.43–0.65 μm and 3.3 – 4.7 μm , with respective average concentrations of $1.2 \times 10^5 \text{ cells m}^{-3} \mu\text{m}^{-1}$ and $1.1 \times 10^5 \text{ cells m}^{-3} \mu\text{m}^{-1}$.

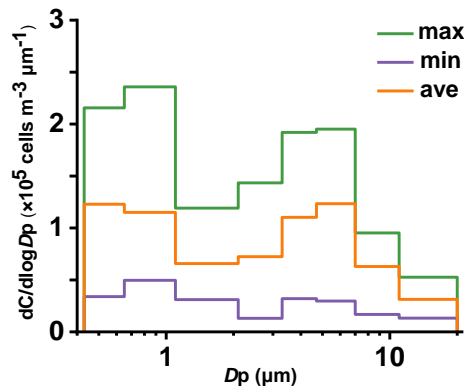


Figure 3-5 Maximum, minimum, and average bacterial aerosols in the eight size ranges in the MIX group (mixed air via long-distance transported air from Asian continent and local emission). Number size distribution of each sample in the MIX group is shown in Fig.S3 (e).

3.3.4 Estimated dry deposition fluxes

The dry deposition fluxes of bacterial cells in fine (0.43–1.1 μm), coarse (1.1–7 μm), and ultra-coarse (>7 μm) size ranges were estimated to reveal the potential importance of the removal processes of bacterial cells according to the particle size ranges. The total dry deposition fluxes of bacteria in LDT, LDM, LSL, LSS, and MIX cases were $4.3 \pm 1.0 \times 10^7$, $2.3 \pm 1.0 \times 10^7$, $7.3 \pm 3.0 \times 10^7$, $2.3 \pm 1.3 \times 10^7$, and $5.6 \pm 3.0 \times 10^7$ cells $\text{m}^{-2} \text{day}^{-1}$, respectively. In the present study, the flux in the LSL cases was the highest, followed by that in the MIX, LDT, and LDM/LSS cases.

Figure 3-6 shows the proportions of the estimated bacterial deposition flux of fine (0.43–1.1 μm), coarse (1.1–7 μm), and ultra-coarse (>7 μm) size ranges. In the LSL cases, the contribution of bacterial cells in coarse and ultra-coarse size ranges (48.5%) was close to that in the fine size range (51.5%). In the LDT cases, more than 90% of bacterial cells deposited in aerosols of the coarse and ultra-coarse size ranges (>1.1 μm) owing to the higher concentration of bacterial aerosols and large size, whose deposition velocities were significantly higher ($P < 0.01$) (Lin et al., 1994) (Lin et al. In the LDM, MIX, and LSS cases, the relative contributions of particles in the range >1.1 μm were similar at 76.9, 70.5, and 76.5%, respectively. These results indicate that terrestrial-derived air masses increased the import of dry deposition of bacterial cells into the receiving environment two-fold compared to marine-derived air masses.

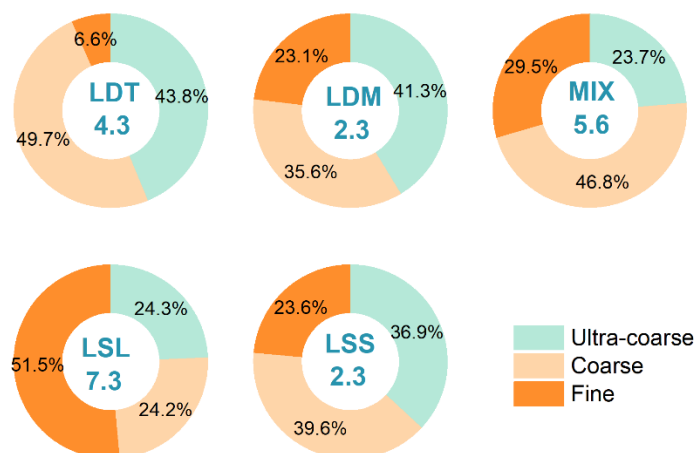


Figure 3-6 Proportion of estimated bacterial deposition flux in LDT (long-distance transported terrestrial air), LDM (long-distance transported marine air), MIX (mixed air via long-distance transported air from Asian continent and local emission), LSL (local-scale land breeze), and LSS (local-scale sea breeze) of fine (0.43–1.1 μm), coarse (1.1–7 μm), and ultra-coarse (>7 μm) size ranges.

3.4 Discussion

3.4.1 Factors determining monomodal and bimodal distributions

The cell concentration and number size distributions of bacterial aerosols at the coastal site varied when the air was controlled by long-distance transported continental air (LDT) and marine air (LDM), by local land breeze (LSL) and sea breeze (LSS), and by the mixing of long-distance transported continental air and local emissions (MIX). The order of the total concentration from highest to lowest was LSL>MIX>LDT>LDM≈LSS. On average, the highest concentration in the entire size range was observed in the LSL cases ($1.9 \pm 1.3 \times 10^5$ cells m⁻³). This was attributed to the massive accumulation of fine bacterial aerosols in the local area under stable weather conditions. The number of cells in the less than 1 μm size range occupied more than half of the total cells in the entire size range. The total bacterial concentration of both LDM and LSS was approximately 0.5×10^5 cells m⁻³, which was the lowest case, indicating the low concentration of bacterial aerosols in marine air, despite the scale of the air parcel movement.

There was a close dependence of the number size distribution of bacterial aerosols in the

atmosphere on the dominance of airflow origins. The distribution showed differences in response to the alternation of terrestrial and marine airflows, which was attributed to the distinctive sources of terrestrial or marine origins. Yin et al. (2021) observed marked differences in the viable bacterial size distribution between air sources originating from the sea and terrestrial regions. Terrestrial air is usually abundant in coarse aerosol particles from natural emissions (usually mineral dust particles) and anthropogenic activities (typical particles from biomass burning, fossil fuel combustion, and road dust). Compared with other long-distance transported terrestrial samples, an increase of 2.2 – 4.1 times in the size range of 3.3 – 4.7 μm was observed in the sample of LDT1. The increase of particle mass in 3.3 – 4.7 μm is a typical characteristic of the occurrence of Asian dust (Han et al., 2004). According to the report of the Japan Meteorological Agency, a dust episode occurred when LDT1 was collected (https://www.data.jma.go.jp/gmd/env/kosahp/kosa_map_20150322.html). These results indicate that the dust particles in the size range of 3.3 – 4.7 μm effectively carried bacteria to the downwind area.

In the present study, the high concentration of bacteria in the LDT cases appeared in the 3.3–4.7 μm size range, an increase of 1.86 compared to the LSL cases. Bacterial cells in the coarse size range also increased when local land breezes prevailed. In the LSL cases, a relatively lower second peak was observed in the size range of 3.3–4.7 μm . The majority of airborne particles in this size range are primary particles, and bacteria exist in cohesion with other particles, namely bacteria attached to other particles. Therefore, the bacterial cells in this range were considered to be dominated by those moving with coarse particles from the Asian continent in the LDT cases and by the emissions from nearby agricultural and farming activities on the island in the LSL cases. Farms in the upwind areas of the land might also contribute to the bacteria in the coarse mode size because particles from cattle feedlots frequently appeared in this size range, and bacteria were abundant (Li et al., 2021). The positive correlation between bacterial aerosols of 3.3–4.7 μm size range and wind speed ($R=0.33$, $P<0.01$) in the LSL indicates that wind was the key factor in mobilizing particles from local surfaces into the air at the island. These results strongly support the idea that the peak mode size in the atmosphere influenced by terrestrial air is closely related to primary particles.

The peak mode in the <1 μm size range occurred only in the air parcels significantly influenced by local terrestrial air, that is, the LSL and MIX cases. Bacteria in this size range are dominated by free-floating cells because of their small size (Hu et al., 2020). The land areas are covered by grasses, trees, and vegetation and are abundant in insects, birds, and small animals,

all of which constantly release bacteria into the air. Therefore, the peak mode occurrence in small areas is likely due to natural emissions from the island.

The bacteria in the air parcels dominated by marine air, that is, in the LDM and LSS cases, should be dominated by sea-surface emissions. In LSS cases, the wind was sometimes extreme. The emission of microbes from surface seawater is closely dependent on the wind; the stronger the wind, the more microbes are emitted (Hu et al., 2017). In addition, some microbes are emitted with sea salt particles, which are frequently in the coarse size range of aerosol particles, and some can be emitted as individual cells. Therefore, the bimodal distribution of bacterial cells in marine air is expected under strong wind conditions. In contrast, when the wind is weak, that is, in the LDM cases, significant emissions of microbes from the sea surface are not anticipated; therefore bacterial concentrations are expected to be very low.

3.4.2 Activation and removal of the bacterial cells in size ranges

Bacterial aerosols play an indispensable role in atmospheric processes. Previous studies have revealed that bacterial aerosols within both continental and marine air masses can act as ice nucleation particles for cloud formation (Bowers et al., 2011; Du et al., 2017). Marine organisms likely contribute to ice nucleation activity at the sea surface microlayer or bulk seawater (Wilson et al., 2015). Bacterial cells in small size ranges have been detected in ice cloud residues (Creamean et al., 2015; Pratt et al., 2009). Particles smaller than 1 μm are usually difficult to remove from the air but have been reported to collide effectively with small droplets (Pöschl et al., 2010) (Pöschl et al., 2010). Similarly, airborne bacterial aerosols in a small size range are difficult to remove from the atmosphere, except for rain washouts. A decrease in removal efficiency by rainfall was observed for particle diameters 0.4 – 10 μm with increasing size, and the majority (55% to 73%) within clouds have been identified as 1 μm microbes (Moore et al., 2020). In the present study, a major proportion (40.5%) of bacterial cells in local breezes of fine size ranges provided cloud nuclei and ice cloud nuclei in clean marine air, and the nuclei were mainly in the fine size ranges. Bacterial cells could be involved in and play a role in precipitation, as some bacteria are known to have nucleation potential for rainfall events (Hu et al., 2017b).

Bacteria in aerosols of coarse size usually exist as aggregations of multiple cells and attach to coarse particles such as mineral dust and marine organic compounds (Woo and Yamamoto, 2020). Coarse bacterial aerosols not only generate large sedimentation velocities and flux densities but also promote cloud formation by serving as cloud condensation nuclei, and the coexistence of

dust and bacterial cells increases the ability of particles to act as ice nuclei for ice crystal formation (Mahowald et al., 2014; Tobo et al., 2013). Proteins in bacteria act as ice nucleation active sites and are well protected when bacteria adhere to mineral dust surfaces (Conen et al., 2015). The concentration of bacterial aerosols in the present LDT cases increased by a factor of 4.6 and 3.8 in the size range of 3.3–4.7 μm and 2.1–3.3 μm , respectively, compared with the LDM cases. Meanwhile, a noticeable fraction (15%) of bacterial aerosols in the LDT cases was detected in the size range $>11 \mu\text{m}$. Because ultra-coarse particles ($>7 \mu\text{m}$) are known to serve as effective giant cloud condensation nuclei (Möhler et al., 2007b), these bacterial aerosols are efficient nuclei for promoting ice cloud formation under appropriate conditions.

Ultra-coarse particles can reach cloud-base altitudes, for example, $>1000 \text{ m}$ (Renard et al., 2018), and bacteria have been implicated in diffusing at cloud-base altitudes (500–2000 m) and even at higher altitudes of the stratosphere (Smith, 2013; Zweifel et al., 2012). Thus, long-distance transport from the continent will significantly increase the concentration of bacterial cells in downwind areas and provide potential nuclei for cloud formation. In addition, terrestrial-derived long-distance air masses occur in spring in westerly winds, resulting in pulse increases of bacterial aerosols in large size ranges providing a substantial amount of aerosol particles in coarse size ranges, favoring ice cloud formation. This is also likely the reason why bacteria are frequently reported to co-exist with mineral dust in clouds.

The estimated dry deposition fluxes of the bacterial cells in different size ranges revealed that terrestrial-derived air masses increased the import of dry deposition of bacterial cells in ultra-coarse aerosols to the recipient environment by two times compared to marine-derived air masses. Bacteria can remain viable after atmospheric transport (Gong et al., 2020), resulting in the wide dispersal of microbes across distant ecosystems. Some bacterial taxa have potential pathogenicity to plants, such as *P. syringae*, with deposition as an essential component in moving to new hosts, leading to risk through the release of toxins and cell wall-degrading enzymes (Monteil et al., 2014). The dry deposition fluxes of bacterial cells in size-differentiated aerosols may affect the structure and function of recipient ecosystems.

3.5 Summary

In this study, we investigated variations in bacterial aerosol size distribution in response to terrestrial versus marine and long-distance versus local airflows. We confirmed that distinctive

airflows could lead to significant differences in the size distribution modes of bacterial aerosols. Coarse bacterial aerosols increased significantly in long-distance air from the Asian continent producing a peak mode size of 3.3 – 4.7 μm , which was supposed to be due to the abundant primary particles in the long-distance transported air. Marine air flows and local sea breezes resulted in uniformly distributed bacterial aerosols with a minimal total cell concentration. The distributions in local land breezes and the air mixed by local land emissions and long-distance transported air was bimodal, with the fine peak mode in the $<1.1 \mu\text{m}$ size range and the coarse mode peak at 3.3 – 4.7 μm . Both mode peaks were supposed to be caused by emissions from the land areas nearby to the site, with the fine mode from the direct emission of microbes and the coarse mode from the emission of coarse primary particles. Results of estimated dry deposition flux of bacterial cells showed that 90% of bacterial cells deposited in aerosols larger than 1.1 μm in cases of terrestrial-derived long-distance transported air. For land breezes, the contributions in the $>1.1 \mu\text{m}$ size range were similar to those in the $<1.1 \mu\text{m}$ size range. These results, which quantitatively show the size-related diffusion characteristics of airborne bacteria in association with synoptic weather conditions, indicate the necessity to consider the size variation of bacterial aerosols according to synoptic weather when studying the roles that bioaerosols play in atmospheric processes. The fundamental information for cell concentrations is provided in this study. Further analyses of bacterial communities in different size ranges will be helpful to the clarification of the mechanisms of size-dependent bacterial aerosols varying with airflows.

Chapter 4

Abundance and viability of particle-attached and free-floating bacteria in dusty and nondust air

4.1 Introduction

As introduced in Chapter 1.1, bacteria-associated aerosols in the air have an aerodynamic diameter significantly larger than the typical size (approximately 1 μm) of individual bacterial cells. This is because airborne bacterial cells are favorably attached to coarse particles, such as dust particles and plant debris, or are sometimes found as assemblages of many cells. In this chapter, the fractions were quantified of particle-attached and free-floating bacterial cells in dusty and nondusty air based on the fact that airborne bacterial cells are usually $\sim 1 \mu\text{m}$ or smaller than 1 μm ; thus, particle-attached bacteria should be trapped in aerosol samples of particles larger than 1 μm , and free-floating bacteria should be located among particles smaller than 1 μm .

By utilizing eight-stage Andersen cascade impactors (Andersen samplers), size-segregated aerosol samples were collected at a southwestern coastal site of Japan in the spring of 2013–2016, when the middle-latitude westerly wind in the Northern Hemisphere frequently brought dust from the Asian continent to the observation site. Viable and nonviable bacteria in each sample were counted using the LIVE/DEAD BacLight bacterial viability assay to estimate bacterial concentrations (Murata and Zhang, 2013, 2016). Bacteria detected in samples of particles larger than 1.1 μm (the cutoff size of the sampler stages) were considered particle-attached bacteria, and those in the stages of particles smaller than 1.1 μm were considered free-floating bacteria. An analysis of method confidence showed that uncertainties due to the sample collection were small (Figures S4-4 and S4-5 in the Supplement). In this study, we focus on comparisons of the quantitative results of particle-attached and free-floating bacteria in the air and the viability of these bacteria under dusty and nondusty conditions.

4.2 Methods

4.2.1 Sample collection and cell enumeration

Aerosol samples were collected on the platform of a building (32.324°N, 129.993°E; 15 m above ground level and 23 m above sea level) on the seaside of Amakusa Island, southwestern Japan (Figure S4-1) during several observational campaigns in the spring of 2013 to 2016. Dust plumes from the Asian continent, called Asian dust, frequently pass this area in spring. There are limited fishery and agriculture activities and few anthropogenic sources of air pollutants around the area, making the site suitable for investigating airborne bacteria in the Asian continental

outflow (Murata and Zhang, 2016).

Aerosol samples were collected onto 0.2 μm pore polycarbonate filters (47 mm; Merck Millipore Ltd., Cork, Ireland) with 8-stage Andersen samplers (Model AN-200; Tokyo Dylec Corp., Japan). The flow rate of the samplers was 28.3 L min^{-1} . Aerosol particles were collected onto 8 filters according to the particle aerodynamic diameter ranges of >11 , 7.0–11, 4.7–7.0, 3.3–4.7, 2.1–3.3, 1.1–2.1, 0.65–1.1 and 0.43–0.65 μm . The collection time of one set of samples was from approximately 3 to 24 h. Details on the sample collection are given in Table 4-1 and Table S4-1 and Figure S4-2 in the Supplement.

Before the collection of each sample set, all stages of the sampler were cleaned carefully, and the plates for the filters were rinsed and wiped with 70% ethanol in a clean hood to avoid contamination. A blank control for each set of samples was prepared, i.e., a blank filter was set in the sampler without sample collection. After sample collection, the filters were sealed in Petri dishes and stored at -20°C until analysis.

The viable and nonviable bacterial cells (Figure S4-3) on the filters were enumerated using the LIVE/DEAD BacLight bacterial viability assay with an epifluorescence microscope (EFM; Eclipse 80i, Nikon Corp., Tokyo, Japan) as described previously (Hu et al., 2017a; Murata and Zhang, 2013, 2016). Bacterial cells and other particles were detached from the aerosol-loaded polycarbonate membranes (47 mm in diameter) in a phosphate-buffered saline solution (PBS, pH 7.4) by vortex shaking and ultrasonic vibration in ice bath. Then the suspension was treated with glutaraldehyde fixation and stained with the LIVE/DEAD BacLight Bacterial Viability Kit (L13152, Invitrogen™, Molecular Probes Inc., Eugene, Oregon, US), followed by filtration on a 25 mm diameter and 0.2 μm pore black polycarbonate membrane for bacterial enumeration. An excitation wavelength range between 450 and 490 nm (blue) was utilized, and the microscope was operated at $1000\times$ magnification. Fluorescent green and red/orange/yellow cells with spherical shape and size close to or smaller than 1 μm in diameter were counted as viable and nonviable bacteria, respectively. There are uncertainties in the bacterial cell counting caused by the LIVE/DEAD BacLight Bacterial Viability Kit because the kit could not distinguish archaea and small eukaryotes including fungi from bacteria (Berney et al., 2007). Since the abundance of archaea and fungi in air could be several (1–6) orders of magnitude less than that of bacteria (Delort et al., 2010; Fröhlich-Nowoisky et al., 2016; Fröhlich-Nowoisky et al., 2014b) and the dominant size range of fungal spores is 2–10 μm (Bauer et al., 2008), the overestimation of bacteria caused by the kit we used should be less than 10% although the uncertainties could not

be quantitatively evaluated. The cell concentrations in the size-segregated particles in the air were estimated based on cell counts and the sampling of air volumes following the subtraction of the blank controls. The viability of a group of bacterial cells was defined as the ratio of the viable bacterial cells to total bacterial cells. The procedure for the experimental operation and the formulations for the estimation of cell concentrations are given in the Supplement (Text S1 in the Supplement).

The collection efficiency of airborne bacterial cells with Andersen samplers was evaluated by comparing the results to those obtained by using BioSamplers (SKC Inc., Eighty-Four, PA, US) and in-line filter holders (47 mm, Millipore Corp., Billerica, MA, US). The comparison shows that the total bacterial concentration results of the Andersen sampler were generally consistent with those of the BioSamplers and the in-line filter holders (Figure S4-4).

4.2.2 Separation of particle-attached and free-floating bacteria

In this study, bacteria in the samples of stages with particles larger than 1.1 μm were considered particle-attached, and bacteria in the samples of stages with particles ranging from 0.43–1.1 μm were considered free-floating. The resuspension of bacteria trapped by upper stages and falling onto lower stages during sample collection may cause uncertainties in the size distribution of bacteria-associated particles and the separation of particle-attached and free-floating bacteria.

The uncertainties in the estimation of particle-attached and free-floating bacteria were investigated in the laboratory (Text S2 in the Supplement). The fractions and concentrations of particle-attached bacteria obtained by the presented method were potentially underestimated. But the underestimation did not significantly affect the size distributions of particle-attached bacteria, and, in particular, the underestimation of the concentrations of particle-attached bacterial cells was less than 10% on average (Figure S4-5). The total bacterial concentration results of the Andersen sampler were generally consistent with those of the in-line filter holders collecting total particles (Figure S4-4). This result indicates that bacteria smaller than 0.43 μm , which are not available by the Andersen samplers in this study, were a minor fraction of the free-floating bacteria.

Table 4-1 Concentration and viability of total, free-floating, and particle-attached bacteria. The concentration of coarse particles (>1 µm) and the ratio of particle-attached bacteria to coarse particles are also listed. The percentages of free-floating and particle-attached bacteria are given in the parentheses. The sample ID indicates the sequence number (1 to 27) of the sample and dust condition (D, dusty; ND, nondusty) and synoptic weather (Pr, prefront; Po, postfront; AA, approaching anticyclone; A, anticyclone) during the sampling period.

Sample ID	Synoptic weather	Coarse particles (10 ⁵ m ⁻³)	Total bacteria		Free-floating bacteria		Particle-attached bacteria (PAB)		
			Concentration (10 ⁵ cells m ⁻³)	Viability (%)	Concentration (10 ⁵ cells m ⁻³)	Viability (%)	Concentration (10 ⁵ cells m ⁻³)	Viability (%)	ration (%)
Dusty (9)									
1D-Pr	Prefront	41	7.8	84	1.7 (21)	90	6.1 (79)	82	15
2D-Po	Postfront	32	2.3	77	0.5 (23)	99	1.8 (77)	71	6
3D-AA	Approaching anticyclone	12	2.2	89	0.7 (30)	91	1.6 (70)	88	13
4D-Pr+Po	Pre-/postfront	52	7.3	61	1.8 (25)	71	5.4 (75)	58	11
5D-AA	Approaching anticyclone	21	4.7	63	0.7 (16)	79	3.9 (84)	60	19
10D-Po	Postfront	16	2.5	40	0.6 (25)	61	1.9 (75)	33	11
17D-AA	Approaching anticyclone	88	2.9	73	1.0 (36)	99	1.9 (64)	59	2

Sample ID	Synoptic weather	Coarse particles (10 ⁵ m ⁻³)	Total bacteria		Free-floating bacteria		Particle-attached bacteria (PAB)		
			Concentration (10 ⁵ cells m ⁻³)	Viability (%)	Concentration (10 ⁵ cells m ⁻³)	Viability (%)	Concentration (10 ⁵ cells m ⁻³)	Viability (%)	ration (%)
26D-Po	Postfront	10	8.2	95	2.5 (30)	97	5.7 (70)	95	59
27D-AA	Approaching anticyclone	15	1.9	87	0.9 (46)	96	1.0 (54)	78	7
Average		32 ± 25	4.4 ± 2.6	74 ± 17	1.2 ± 0.7 (28 ± 9)	87 ± 14	3.2 ± 2.1 (72 ± 9)	69 ± 19	16 ± 17
Nondust (18)									
6ND-AA	Approaching anticyclone	13	1.5	75	0.4 (27)	88	1.1 (73)	70	9
7ND-A	Anticyclone	12	1.5	74	0.6 (39)	82	0.9 (61)	69	8
8ND-A+Pr	Anticyclone+prefront	14	0.8	98	0.2 (31)	99	0.5 (69)	98	4
9ND-Pr	Prefront	26	2.7	73	1.9 (71)	84	0.8 (29)	45	3
11ND-AA	Approaching anticyclone	4	2.1	72	1.3 (64)	85	0.8 (36)	51	18
12ND-A	Anticyclone	14	2.9	83	2.1 (73)	96	0.8 (27)	48	6
13ND-A	Anticyclone	9	3.6	75	2.5 (70)	86	1.1 (30)	50	12
14ND-A	Anticyclone	13	1.9	77	0.8 (42)	99	1.1 (58)	62	9

Sample ID	Synoptic weather	Coarse particles (10 ⁵ m ⁻³)	Total bacteria		Free-floating bacteria		Particle-attached bacteria (PAB)		
			Concentration (10 ⁵ cells m ⁻³)	Viability (%)	Concentration (10 ⁵ cells m ⁻³)	Viability (%)	Concentration (10 ⁵ cells m ⁻³)	Viability (%)	ration (%)
16ND-Po	Postfront	16	2.5	89	0.9 (35)	96	1.6 (65)	85	10
18ND-AA	Approaching anticyclone	15	2.9	91	0.5 (18)	86	2.4 (82)	92	16
19ND-A	Anticyclone	9	1.1	72	0.4 (35)	96	0.7 (65)	59	7
20ND-A	Anticyclone	10	1.0	77	0.4 (41)	85	0.6 (59)	72	6
21ND-A	Anticyclone	13	1.7	63	1.0 (63)	89	0.6 (37)	18	5
22ND-A	Anticyclone	8	1.2	40	0.5 (43)	56	0.7 (57)	28	9
23ND-Pr+Po	Pre-/postfront	12	1.1	59	0.5 (48)	88	0.6 (52)	32	5
24ND-Po+A	Postfront/Anticyclone	7	1.4	72	0.5 (38)	88	0.8 (62)	62	12
25ND-A	Anticyclone	6	1.5	85	0.6 (40)	95	0.9 (60)	78	15
Average		12 ± 5	2.0 ± 1.0	75 ± 13	0.9 ± 0.7 (44 ± 17)	87 ± 12	1.1 ± 0.7 (56 ± 17)	60 ± 22	10 ± 7
All (27)									
Average		18 ± 18	2.8 ± 2.0	74 ± 14	1.0 ± 0.7 (39 ± 16)	87 ± 12	1.8 ± 1.7 (61 ± 16)	63 ± 21	12 ±

4.2.3 Atmospheric conditions

During the observation periods, the number concentrations of size-segregated airborne particles (>0.3 , >0.5 , >1.0 , >2.0 , and >5.0 μm in diameter) were monitored with optical particle counters (OPC, KC-01D in 2013 and KC-01E in 2014–2016, Rion Co., Ltd, Tokyo, Japan). In this study, fine particles are in the range of 0.3–1.0 μm , and those larger than 1.0 μm are referred to as coarse particles. Meteorological conditions, including temperature, pressure, relative humidity, precipitation, and wind speed and direction, were monitored with a weather transmitter (WXT520, Vaisala Inc., Helsinki, Finland). Airborne particle number concentrations and meteorological data during the observation periods are summarized in Fig. S4-2 and Table 4-1.

On the basis of surface pressure and weather charts in the days before and after sample collection (Figures S4-2 and S4-6), the air parcels on the synoptic scales from which samples were collected were categorized into four groups: prefront, postfront, approaching anticyclone, and anticyclone (Table 4-1 and S4-1). Details of the categorization are available in Murata and Zhang (2016).

Dust episodes were identified by significant increases in coarse particle concentrations (>1 μm), the forecast for Asian dust distributions in the east Asian region (<http://www-cfors.nies.go.jp/~cfors/>; Figure S4-7), and the backward trajectory of air masses calculated with the NOAA hybrid single-particle Lagrangian integrated trajectory (HYSPLIT) model (http://ready.arl.noaa.gov/HYSPLIT_traj.php). During dust events, the coarse particle concentration largely increased at the study site (Zhang et al., 2003). Dust particles were present in the postfront air and sometimes in the approaching anticyclone air. The results of backward trajectory analysis during dusty and nondust episodes are shown in Figure S4-8.

4.3 Results

4.3.1 Concentrations of airborne bacteria in segregated size ranges

The concentrations of bacterial cells, including viable and nonviable cells, generally showed a bimodal number-size distribution during dust episodes (e.g., Figure 4-1*a, b, d, f*). Most of the bacteria were present in particle fractions with aerodynamic size (D_p) ranges larger than 2 μm (i.e., 2.1–3.3, 3.3–4.7 and 4.7–7.0 μm ; Figure S4-9). These sizes are larger than the size of individual airborne bacterial cells (approximately 1 μm or smaller), indicating that the bacteria

did not float individually in the air but were combined with other particles or were agglomerates of bacterial cells, i.e., the bacteria were particle-attached. The agglomerates of bacterial cells usually appear near emission sources, e.g., sea spray and leaf water (Lighthart, 1997), and probably contributed a limited portion to particle-attached bacteria in this study. There were also many bacterial cells in the size ranges smaller than 1.1 μm , i.e., free-floating bacterial cells. Their concentration was comparable to or lower than the concentrations of bacteria in the larger size ranges (Figures 4-1 and S4-9).

In contrast to dust episodes, during nondust periods, the number-size distribution of bacteria largely varied and did not show any trend with respect to weather conditions. In six cases during nondust periods (9ND-Pr, 11ND-AA, 12ND-A, 13ND-A, 14ND-A, and 21ND-A; Figure S4-9), the bacteria appeared mainly in size ranges smaller than 1.1 μm and accumulated the most in the size range of 0.43–0.65 μm (e.g., Figure 4-1c), indicating the predominance of free-floating bacteria. During most of the other nondust periods (6ND-AA, 7ND-A, 8ND-A+Pr, 16ND-Po, 19ND-A, 20ND-A, 22ND-A, 23ND-Pr+Po, 24ND-Po+A, and 25ND-A), the distributions of bacteria were similar to those during the dust periods, although the concentrations were much lower than or comparable to those in the dust episodes (e.g., Figure 4-1e). There were two exceptional cases in nondust periods that had a mono-modal distribution, with peaks at 3.3–4.7 μm (15ND-AA) or larger than 11 μm (18ND-AA) (Figure S4-9). Multiple processes including advection, deposition, local emission and local convective mixing could influence the size distributions. Unfortunately, we do not have enough case data to investigate statistically meaningful connections between the size distribution and those processes.

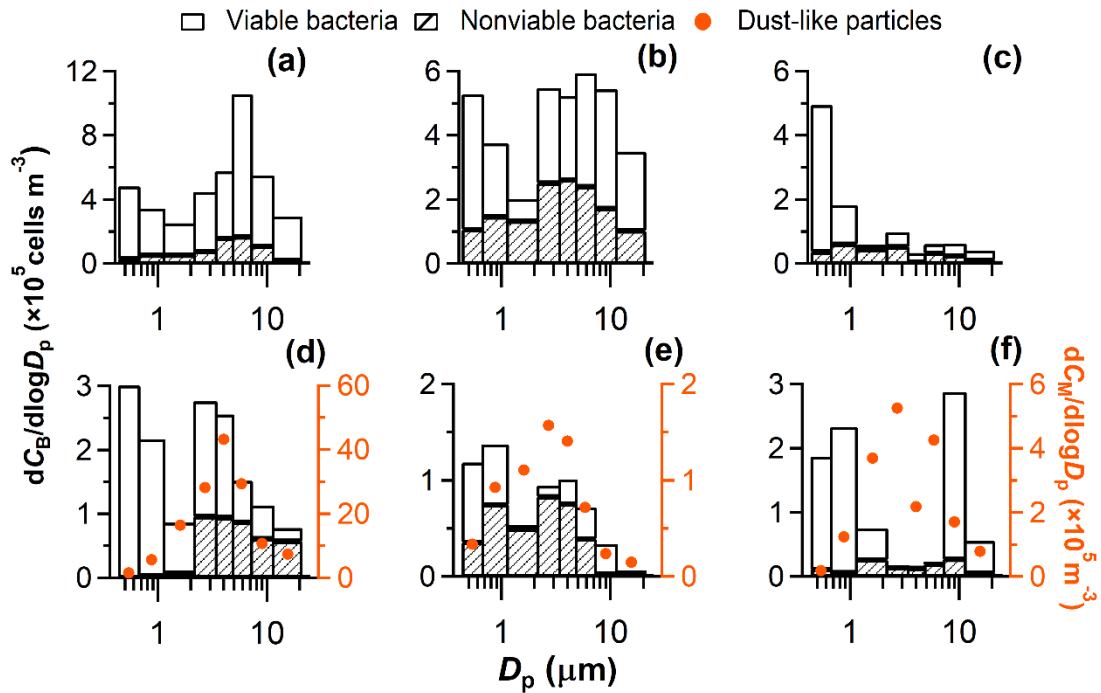


Figure 4-1 Concentrations of viable and nonviable bacteria (C_B) and mineral dust-like particles (C_M) in size-segregated airborne particles. Selected samples are shown as examples: (a) 1D-Pr; (b) 4D-Pr+Po; (c) 11ND-AA; (d) 17D-AA; (e) 22ND-A; (f) 27D-AA. The results of all sampling periods are depicted in Figure S4-9 in the Supplement.

4.3.2 Concentration of particle-attached and free-floating bacteria

The report of results when data are non-normal distribution should be viewed with caution, since many statistical analyses (e.g., the average and standard deviation) are only applicable to random samples from populations with a normal distribution. Aerobiological data possibly do not have a normal distribution (Kasprzyk and Walanus, 2014; Limpert et al., 2008). Whereas, in this study, to make the comparisons among the values easily understood and avoid misunderstanding, we assume the data are normally distributed.

On average, the concentration of total bacterial cells, $4.4 \pm 2.6 \times 10^5 \text{ cells m}^{-3}$, during dust episodes was more than twice that during nondust periods, $2.0 \pm 1.0 \times 10^5 \text{ cells m}^{-3}$ (Table 4-1). This large difference (independent samples t test, $p < 0.05$) in concentration is consistent with the results of previous studies (Hara and Zhang, 2012; Yamaguchi et al., 2014). The concentrations of particle-attached bacterial cells during dust episodes and nondust periods were $3.2 \pm 2.1 \times 10^5$

and $1.1 \pm 0.7 \times 10^5$ cells m^{-3} , respectively. During dust periods particle-attached bacteria accounted for $72 \pm 9\%$ of total bacterial counts, while during nondust periods particle-attached bacteria occupied much lower proportions of $56 \pm 17\%$ (independent samples *t* test, $p < 0.05$). These results suggest that dust particles carry a substantial amount of bacterial cells on their surfaces from dust source areas to remote downstream areas.

On the other hand, the percentage of free-floating bacterial cells was in some cases higher than 70% during nondust periods (Table 4-1). In particular, the percentage ranged from 35% to 73% ($49 \pm 15\%$ on average) under anticyclone weather conditions, when the air mass moved sluggishly and was mainly influenced by marine and local emissions and less by continental emissions (Figure S4-8). Therefore, a substantial fraction of airborne bacteria were free-floating, and they were frequently the common bacteria in nondust air.

The number ratio of particle-attached bacteria to particles in the size range larger than $1.1 \mu m$ was $12 \pm 11\%$ on average (Table 4-1). Except for two periods when the ratios were 35% and 59%, respectively, the ratio was approximately stable ($9 \pm 5\%$ on average for the other periods), regardless of dust episodes and nondust periods (Table 4-1). That is, assuming that a bacteria-attached coarse particle harbors at least one bacterial cell, coarse particles including mineral dust particles with attached bacteria usually made up less than 9% of the total coarse particles. Maki et al. (2008) reported that the mineral particles with attached bacteria made up approximately 10% of the total mineral particles, with the remaining mineral particles possessing few or no bacterial cells at 800-m height above the ground in an Asian dust source region, Dunhuang, China.

The number-size distributions of bacterial cells and mineral dust-like particles (insoluble and with irregular shapes; Figure S4-3) in the microscope fields of some samples were compared. In most cases, the size distributions (mode sizes) of mineral dust-like particles and bacteria in the size ranges larger than $1.1 \mu m$ showed very good consistency (Figures S4- 1 and S4-9). In some cases, the concentration of bacteria in the size ranges larger than $1.1 \mu m$, especially nonviable bacteria, was closely correlated with the mineral dust-like particles in the size-segregated samples (Fig. 2). These results further confirm that the bacteria observed in the large size ranges were closely associated with airborne coarse particles, i.e., they were particle attached. In some cases, the mode size ranges of the bacterial cells and the dust-like particles were inconsistent (Figure S4-9), likely because the number of bacteria on the surface of each coarse particle largely varied or there were less dust-like particles in the coarse size ranges (e.g., 26D-Po). Dust-like particles were rarely observed in the size ranges smaller than $1.1 \mu m$ (Figure S4-9), further indicating that

the bacteria observed in those size ranges were predominantly free-floating.

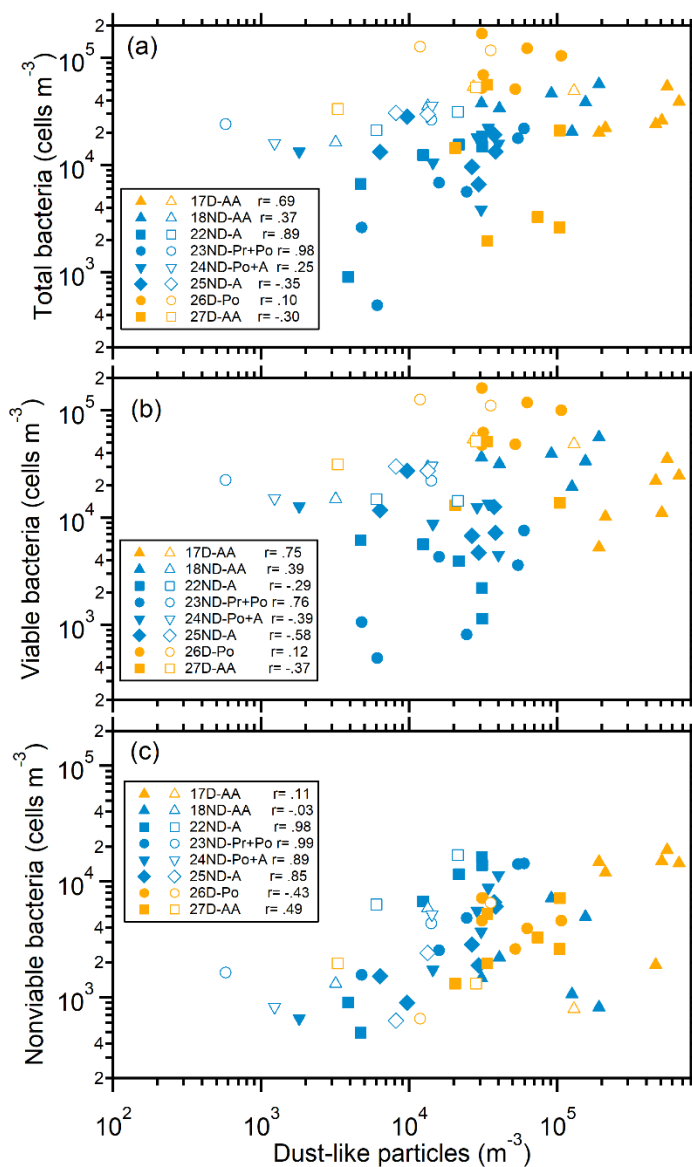


Figure 4-2 Relationship between bacteria and mineral dust-like particles in size-segregated aerosols. (a) Total bacteria, (b) viable bacteria, and (c) nonviable bacteria. Solid and open circles represent particles in the size ranges larger and smaller than $1.1\ \mu m$, respectively. The Pearson correlation coefficients (r) between bacteria and mineral dust-like particles for particles larger than $1.1\ \mu m$ are shown.

4.3.3 Viabilities of particle-attached and free-floating bacteria

The viability of particle-attached bacteria varied over a wide range from 18% to 98% ($63 \pm 21\%$ on average), and the viability of free-floating bacteria was between 56% and 99% ($87 \pm 12\%$ on average) (Table 4-1), much higher than the viability of particle-attached bacteria (Paired samples *t* test, $p=0.00$). The attachment of airborne bacteria to larger particles is expected to be favorable for retaining the viability or cultivability of cells and may indirectly increase the diversity of bacterial communities because of the possible protection of bacterial cells from harsh atmospheric conditions (Bowers et al., 2013; Lighthart, 2000; Prospero et al., 2005).

However, we found that the viability of particle-attached bacteria tended to be lower than that of free-floating bacteria, regardless of weather conditions (Table 4-1). This result indicates that a fraction of the particle-attached bacterial cells were either nonviable when they were blown into the air with the dust or had experienced atmospheric stressors for several days during long-distance transport and changed from a viable to a nonviable state. This is also likely the reason for the poor correlation (Pearson correlation $r=0.35$, $p=0.075$) between the viability of particle-attached bacteria and the ratio of particle-attached bacteria to coarse particles (Table 4-1). In contrast, a large fraction of free-floating bacteria were viable. A fraction of these bacteria were likely from local areas, with a residence time (usually less than one day) shorter than that (2–3 days) of the particle-attached bacteria transported from the Asian continent (Figure S4-8). The proportion of free-floating bacteria was higher under nondust conditions when the air masses moved slowly above the marine area. However, for special cases, such as the one of 20ND-A when the air was from the north due to the specific weather of west-high pressure versus east-low pressure in the westerly, a substantial fraction of the bacteria could be from the local and close areas due to the extremely strong wind. In terms of concentration, viable particle-attached bacteria were usually more abundant than viable free-floating bacteria in dust episodes (Figure S4-1 and S4-9).

On average, the viability ($74 \pm 17\%$) of total bacteria in dusty episodes was close to the viability ($75 \pm 13\%$) of total bacteria during nondust periods (Table 4-1). The viability of particle-attached bacteria ($69 \pm 19\%$) during dust periods was slightly higher than that ($60 \pm 22\%$) during nondust periods. The majority of particle-attached bacteria were viable.

Free-floating bacteria exhibited a quite high viability, and the viabilities of the bacteria in dusty ($87 \pm 14\%$ on average) and nondust ($87 \pm 12\%$) air were similar. The concentration of viable free-floating bacteria was 3.8×10^4 – 1.5×10^5 cells m^{-3} , which was lower than that of particle-

attached bacteria (6.2×10^4 – 5.1×10^5 cells m^{-3}). An increase in viable free-floating bacteria on the order of 10^5 cell m^{-3} (1.1 – 2.2×10^5 cell m^{-3}) was observed when the weather was fine and the air masses moved slowly from marine areas (e.g., 9ND-Pr, 12ND-A, and 13ND-A), favoring the accumulation of bacteria emitted from local areas (Figure S4-8).

4.4 Discussion

4.4.1 Implication from the comparison with literature data

There are few data on airborne bacterial cells available for comparison with the present study. Observations in the multiphase atmosphere with culture-dependent methods revealed that approximately 60–90% or even more culturable airborne bacteria were present in the size range of particles larger than $1.1 \mu m$ (Agarwal, 2017; Burrows et al., 2009b; Montero et al., 2016; Raisi et al., 2013), and the median aerodynamic diameter of particles containing culturable bacteria was approximately 2–4 μm at diverse sites (Lighthart, 2000; Raisi et al., 2013; Shaffer and Lighthart, 1997; Tong and Lighthart, 2000). These results indicate the predominance of culturable particle-attached bacteria in the air, which is approximately in line with the results under dusty and nondust conditions of this study.

Early studies with single-particle analysis frequently encountered the mode size of biological aerosol particles in the size range smaller than $1 \mu m$ (Matthias-Maser et al., 1999; Matthias-Maser and Jaenicke, 1995, 2000). In contrast, recent real-time measurements using ultraviolet aerodynamic particle sizer spectrometers and wideband integrated bioaerosol sensor techniques revealed the mode size of fluorescent biological aerosol particles (FBAP) to be approximately 2–6 μm , and the particles were mainly attributed to fungal spores (Huffman et al., 2010; Pöschl et al., 2010; Savage et al., 2017; Yue et al., 2017). However, the abundant particle-attached bacteria identified in this study in size ranges larger than $2 \mu m$ indicate dust-particle-attached bacteria should not compose small fractions of real-time FBAP results in the relevant size ranges. In addition, the mode at or smaller than $1 \mu m$ observed in real-time FBAP studies is likely consistent with the presence of free-floating bacterial cells in the present study, but the comparison and discussion on the data are not confident because of the large uncertainties caused by the low counting efficiency and accuracy in submicron size ranges of the instruments used in the studies (Huffman et al., 2010; Yue et al., 2017).

Since there are rare other equivalent data for comparison, we discuss the influences of

airborne bacteria according to the results obtained in this study and relevant general understandings in the following subsections.

4.4.2 Ice cloud formation

Dust particles from desert areas are constantly spread at local, regional and global scales in the atmosphere. These particles transport microorganisms across continents and oceans to remote downstream areas (Griffin, 2007; Schuerger et al., 2018). It has been shown that bacteria in the air are more effective ice nuclei at temperatures up to -2°C than abiotic particles (Ariya et al., 2009b; Burrows et al., 2013; Fröhlich-Nowoisky et al., 2016; Möhler et al., 2007a). Biological particles coexisting with dust particles have been detected in ice residues sampled from clouds (Creamean et al., 2013; Pratt et al., 2009), and the coexistence of dust and bacterial cells increases the ability of particles to act as ice nuclei for ice crystal formation (Tobo et al., 2019). Proteins in bacteria are ice nucleation active sites and are well protected when bacteria adhere to mineral dust surfaces (Conen et al., 2011). The attachment of bacteria to dust particles possibly increases the number of sites for ice nucleation and consequently the ice nucleation ability of dust particles (Augustin-Bauditz et al., 2016; Boose et al., 2019; Conen et al., 2011). The present results show that up to one-tenth or more dust particles could be bacteria carriers, and the concentration of particle-attached bacteria, i.e., the number of bacteria-dust contact sites in dust episodes, was on average 3 times larger than that during nondust periods (Table 4-1). The occurrence of dust in remote downstream areas will significantly increase not only the concentration of bacterial cells but also the concentration of dust-bacteria mixture particles and the number of ice nucleation active sites. This phenomenon could provide important sources of nuclei for ice cloud formation under saturated meteorological conditions for icing, particularly in remote elevated air, where the concentrations of aerosol particles able to act as nuclei are usually very low (Creamean et al., 2013).

4.4.3 Ecosystem conservation and development

More than 60% of particle-attached bacteria and approximately 87% of free-floating bacteria in the dusty air remained viable. Airborne bacteria can multiply more easily after they settle into water (lakes, rivers and oceans) and soil surfaces than in the atmosphere. As a consequence, their dissemination via the atmosphere has the potential to alter the microbial biogeography, biogeochemistry and ecosystem services of downstream areas. Moreover, a recent study on phosphorus in aerosol particles in Asian continental outflow revealed that natural dust particles supplied higher ratios of bioavailable phosphorus than other types of particles as nutrients for the

primary production in marine ecosystems, and the phosphorus was presumed to be from the biological particles in dust plumes (Shi et al., 2019). The dissemination of bacteria with dust in the air is much more efficient than that via other routes, such as rivers, because dust in the atmosphere can travel globally within two weeks (Uno et al., 2009). Therefore, the wide dispersal of atmospheric dust is an efficient link between bacterial communities in geographically isolated ecosystems. This linking function is likely the key process that constantly blurs the distinctions between closely related microbial species in distant areas. Thus, the diversities of microorganisms have a geographically weak gradient at the global scale, and are functions of habitat properties but not of historical/evolutionary factors (Fenchel and Finlay, 2004).

4.4.4 Health effects

Allergenic and toxic bacteria inhaled and deposited on the surface of upper respiratory tracts and lungs are suggested to provoke severe adverse health effects, regardless of whether the bacteria are viable, dead or cell fragments (Després et al., 2007; Fröhlich-Nowoisky et al., 2016). Dust particles carrying biological materials, including bacteria with pathogenic, allergenic, and adjuvant activity, can cause and aggravate respiratory disorders (Reinmuth-Selzle et al., 2017). The size distribution of bacteria-related particles in the air is particularly meaningful because the movement and deposition of the particles in the airways are size-dependent. Particles larger than 0.5 μm are deposited by sedimentation and impaction mainly in the head airways, and particles smaller than 0.5 μm can reach the lower airways by diffusion (Fröhlich-Nowoisky et al., 2016). According to the size distribution of the airborne bacteria-related particles in this study (Figures 4-1 and S4-9), the deposition fraction and abundance of particle-attached bacteria are much higher than those of individual cells in both the upper and the lower airways. Polymenakou et al. (2008) reported that a large fraction of airborne bacteria at respiratory particle sizes ($< 3.3 \mu\text{m}$) during an intense dust event were phylogenetic neighbors to human pathogens. He et al. (2012) suggested that Asian dust caused the exacerbation of pneumonia induced by *Klebsiella pneumoniae* due to the enhanced production of pro-inflammatory mediators in alveolar macrophages. Therefore, free-floating bacterial cells are likely to more easily influence the deep parts than the upper parts of respiratory airways, while the negative influence of particle-attached bacteria, particularly under dust conditions, is expected to be more serious in the upper parts than in the deep parts of respiratory airways.

4.5 Conclusions

In this study, we aimed to quantify the particle-attached and free-floating bacteria in dusty and nondust air in southwestern Japan using the fluorescent enumeration of bacterial cells in size-segregated aerosol samples. The bacteria showed bimodal number-size distributions during dust episodes, while the distributions largely varied during nondust periods. Particle-attached bacteria in dust episodes, with a concentration of $3.2 \pm 2.1 \times 10^5$ cells m^{-3} on average, occupied 72 ± 9 % of the total bacteria. In contrast, this percentage was 56 ± 17 % during nondust periods, with a concentration of $1.1 \pm 0.7 \times 10^5$ cells m^{-3} . The results indicate that dust particles conveyed substantial numbers of bacterial cells on their surfaces. Viable particle-attached bacteria were more abundant than viable free-floating bacteria in dusty air, which is compatible with the previous results that larger particles harbor more viable and/or culturable bacteria than smaller particles.

The viability (approximately 63 ± 21 %) of particle-attached bacteria was much lower than that (87 ± 12 %) of free-floating bacteria, likely because atmospheric stressors along with long-distance transport inhibited the survival of particle-attached bacteria and the entrainment of locally originating free-floating bacteria. High concentrations and viabilities of free-floating bacteria were observed in stagnant air, mostly under anticyclone conditions, suggesting that locally emitted bacteria accounted for the major fractions.

The present results, quantitatively showing the state of airborne bacteria in association with particles, i.e., particle-attached and free-floating bacteria, could have broad implications in the disciplines of atmospheric sciences, ecology, public health and climate. In addition, the methods used in this study are low cost and easily available but are time- and labor-intensive. Verification of the status of airborne bacteria using efficient techniques, such as *in situ* electron microscopy, and the exploration of the compositions, functions and activities of particle-attached and free-floating bacteria in the atmosphere, are necessary to deepen our understanding of the related fields.

Chapter 5

Conclusions and perspectives

The size distribution has an essential place in the transit and life cycle of bacterial aerosols in the atmosphere. The aerodynamic size of bacterial aerosols determines their transportation ability, the capability for atmospheric reaction, and the deposition velocity. It is therefore important to characterize the size distribution and clarify the transit dynamics of bacterial aerosols.

In this study, firstly the uncertainties of Andersen sampler for extended sampling duration were examined. Results showed that the concentration of bacterial cells in the size range of $> 4.7 \mu\text{m}$ could be underestimated 40 - 50% as the concentration in the size range smaller than $3.3 \mu\text{m}$ was overestimated when the sample collection time was more than 6 hours. Sample collection time should be less than 20 minutes to suppress the uncertainty below 10%, and 42 minutes to smaller than 20%. Based on identified exponential inverse relation between the dropping rate from each stage and sample collection time, a scheme is proposed to calibrate the counting results of Andersen sampler samples to obtain the number size distribution of airborne bacterial cells with examples.

Number size distribution was measured under various airflows using the Andersen sampler with the calibration scheme. It was found that the distribution in the long-distance transported terrestrial air from the Asian continent was monomodal, with a peak of $3.3\text{--}4.7 \mu\text{m}$. The distribution in local land breeze air was bimodal, with the peaks at $0.43\text{--}1.1$ and $3.3\text{--}4.7 \mu\text{m}$. A similar bimodal distribution was encountered when the local island air and long-distance transported terrestrial air mixed. In contrast, the size distribution did not show clear peaks in the air from either nearby or remote marine areas. The estimation of dry deposition fluxes of bacterial cells showed that the deposition was dominated by cells larger than $1.1 \mu\text{m}$ with a relative contribution from 70.5% to 93.7%, except for the local land breeze cases, where the contributions in the size ranges larger and smaller than $1.1 \mu\text{m}$ were similar.

The concentration of particle-attached bacteria ($> 1 \mu\text{m}$), and free-floating bacteria ($< 1 \mu\text{m}$) revealed that dust particles carried substantial amounts of bacteria on their surfaces, more than half of which were viable, and spread these bacteria through the atmosphere. These results show the distinctive number size distributions and removal processes of bacterial aerosols in different types of air. In addition, they indicate that size-dependent characteristics of airborne bacteria should be considered when studying their activities and roles in the atmospheric environment.

The information given in this study provide new understandings on the dependence of synoptic weather systems on size distribution of bacterial aerosols. However, related investigation is still at infancy and further prospects for the future can be conducted to obtain more insights

about the roles of bacterial aerosol in physics and chemistry of the atmosphere as follows:

1. More attention is needed to understand the success of size-related taxa at being transferred to aerosols and surviving in the atmosphere (cell size and density, pigments, composition of the cell membrane), as this success expresses a potential to invade or exchange new environments. A better characterization of the specific features of microorganisms adapted to the atmospheric environment, and the identification of specific indicators, would also be particularly necessary.

2. Combining with microbial indicators specific for the different sources may be helpful to understand the factors that shape the microbial content and the microbial diversity in atmosphere and facilitate prevention from health and microecosystem impacts. One final prospect is to quantify the impact of human activities and climate changes on the sources associated bioaerosols, and possibly transport modelling related to the size.

3. The size effect of bacterial aerosols on clouds and the climate is still faced to uncertainties related to cloud formation and their microphysical and metabolism properties, which are highly variable in time and space. One factor contributing to these uncertainties is the current lack of knowledge on bacterial interference in chemistry processes in clouds. Cloud chemistry studies are therefore crucial for scientists to evaluate the effects of clouds on climate change. The complex nature of cloud microphysical and size dynamic processes will require robust parameterizations to be developed to represent various potential bacterial INP behavior, for implementation in simulations from cloud to regional to global scales.

4. Transport models involved in size have proven very useful to many applications in simulating the atmospheric dispersal of several types of biotic particles over a whole range of scales, from the plant to the globe. The different modeling approaches considered now appear to be well adapted to bioaerosol-related transit and are complementary. As microbial aerosols travel over a continuum of scales, which the current models have not taken into account well. Models should be developed for the transport of biological particles.

Acknowledgements

Firstly, my utmost gratitude runs to Prof. Zhang, whose guidance, patience, support, and commitment for my study here. I really value the study time under the supervision of Prof. Zhang and he has shown me, by his example, what a good and professional scientist should be.

I would also like to express my sincere appreciations to Profs. Ishibashi Yasuhiro, Matsusaki Hiromi, and Shiratsuchi Hideki for the advice, support, and directions in my academic life here.

I would like to send my thanks to Prof. Wei Hu, who help a lot in my research and set a really great example for me, and I have been inspired and motivated. Special thanks to Prof. Tomoko Kojima for leading our weekly seminars at Prefectural University of Kumamoto. I would like to also thank Ms. Remi Inamura and Ms. Ayumi Naganuma for administrative supports.

Thanks for all the past and current members in AERL for help and supports in my life living in Japan. We share a lot of interesting memories.

Again, thanks for cohort members Drs. Wenwen Xie, Wenshuai Li, Long Zhang, Mr. Yalou Wang, and Mr. Taisei Touyama, we spent plenty of lovely times on academical discussion and wonderful moments in daily life. Thanks to all the international friends I met in Japan and for our memorable moments. Special thanks to Dr. Pyae Sonesoe, whose mental support, daily care, life inspiration, and academic encouragement have motivated me widely. Let's do our best!

To my entire family, and all of my loved friends in China, I highly appreciate for their support and encouragement. Especially, appreciations and forever respect to my great father, who always encouraged me to pursue for academic achievement, and I wish him to be showered with blessings and eternal joy.

Thanks for China Scholarship Council (No. 201906560020) to support my stay at the Prefectural University of Kumamoto, Japan. Finally, the author of this dissertation would like to acknowledge and declare that the research work reported was done at Graduate School of Environmental and Symbiotic Science, Prefectural University of Kumamoto, and this research work has not been submitted for any other degree.

References

- Agarwal, S., 2017. Seasonal variability in size-segregated airborne bacterial particles and their characterization at different source-sites. *Environmental Science and Pollution Research* 24, 13519-13527.
- Ahern, H., Walsh, K., Hill, T., Moffett, B., 2007. Fluorescent pseudomonads isolated from Hebridean cloud and rain water produce biosurfactants but do not cause ice nucleation. *Biogeosciences* 4, 115-124.
- Alsved, M., Bourouiba, L., Duchaine, C., Löndahl, J., Marr, L.C., Parker, S.T., Prussin, A.J., Thomas, R.J., 2020. Natural sources and experimental generation of bioaerosols: Challenges and perspectives. *Aerosol Science and Technology* 54, 547-571.
- Amato, P., 2012. Clouds Provide Atmospheric Oases for Microbes. *Microbe* 7, 119-123.
- Amato, P., Joly, M., Besaury, L., Oudart, A., Taib, N., Mone, A.I., Deguillaume, L., Delort, A.M., Debross, D., 2017. Active microorganisms thrive among extremely diverse communities in cloud water. *PLOS ONE* 12, e0182869.
- Amato, P., Ménager, M., Sancelme, M., Laj, P., Mailhot, G., Delort, A.-M., 2005. Microbial population in cloud water at the Puy de Dôme: implications for the chemistry of clouds. *Atmospheric Environment* 39, 4143-4153.
- Andersen, A.A., 1958. New sampler for the collection, sizing, and enumeration of viable airborne particles. *Journal of Bacteriology* 76, 471-484.
- Ariya, P., Sun, J., Eltouny, N., Hudson, E., Hayes, C., Kos, G., 2009a. Physical and chemical characterization of bioaerosols—Implications for nucleation processes. *International Reviews in Physical Chemistry* 28, 1-32.
- Ariya, P.A., Amyot, M., Dastoor, A., Deeds, D., Feinberg, A., Kos, G., Poulain, A., Ryjkov, A., Semeniuk, K., Subir, M., Toyota, K., 2015. Mercury physicochemical and biogeochemical transformation in the atmosphere and at atmospheric interfaces: a review and future directions. *Chem Rev* 115, 3760-3802.
- Ariya, P.A., Sun, J., Eltouny, N.A., Hudson, E.D., Hayes, C.T., Kos, G., 2009b. Physical and chemical characterization of bioaerosols – Implications for nucleation processes. *International Reviews in Physical Chemistry* 28, 1-32.
- Augustin-Bauditz, S., Wex, H., Denjean, C., Hartmann, S., Schneider, J., Schmidt, S., Ebert, M., Stratmann, F., 2016. Laboratory-generated mixtures of mineral dust particles with biological substances: characterization of the particle mixing state and immersion freezing behavior.

Atmospheric Chemistry and Physics 16, 5531-5543.

Aylor, D.E., 1986. A framework for examining inter-regional aerial transport of fungal spores. *Agricultural and Forest Meteorology* 38, 263-288.

Bauer, H., Claeys, M., Vermeulen, R., Schueller, E., Weinke, G., Berger, A., Puxbaum, H., 2008. Arabitol and mannitol as tracers for the quantification of airborne fungal spores. *Atmospheric Environment* 42, 588-593.

Berney, M., Hammes, F., Bosshard, F., Weilenmann, H.U., Egli, T., 2007. Assessment and interpretation of bacterial viability by using the LIVE/DEAD BacLight Kit in combination with flow cytometry. *Appl Environ Microbiol* 73, 3283-3290.

Boose, Y., Baloh, P., Plötze, M., Ofner, J., Grothe, H., Sierau, B., Lohmann, U., Kanji, Z.A., 2019. Heterogeneous ice nucleation on dust particles sourced from nine deserts worldwide – Part 2: Deposition nucleation and condensation freezing. *Atmospheric Chemistry and Physics* 19, 1059-1076.

Bowers, R.M., Clements, N., Emerson, J.B., Wiedinmyer, C., Hannigan, M.P., Fierer, N., 2013. Seasonal variability in bacterial and fungal diversity of the near-surface atmosphere. *Environ Sci Technol* 47, 12097-12106.

Bowers, R.M., McCubbin, I.B., Hallar, A.G., Fierer, N., 2012. Seasonal variability in airborne bacterial communities at a high-elevation site. *Atmospheric Environment* 50, 41-49.

Bowers, R.M., McLetchie, S., Knight, R., Fierer, N., 2011. Spatial variability in airborne bacterial communities across land-use types and their relationship to the bacterial communities of potential source environments. *ISME J* 5, 601-612.

Burrows, S.M., Butler, T., Jöckel, P., Tost, H., Kerkweg, A., Pöschl, U., Lawrence, M.G., 2009a. Bacteria in the global atmosphere—Part 2: Modeling of emissions and transport between different ecosystems. *Atmospheric Chemistry and Physics* 9, 9281-9297.

Burrows, S.M., Elbert, W., Lawrence, M.G., Pöschl, U., 2009b. Bacteria in the global atmosphere—Part 1: Review and synthesis of literature data for different ecosystems. *Atmospheric Chemistry and Physics* 9, 9263-9280.

Burrows, S.M., Hoose, C., Pöschl, U., Lawrence, M.G., 2013. Ice nuclei in marine air: biogenic particles or dust? *Atmospheric Chemistry and Physics* 13, 245-267.

Cao, C., Jiang, W., Wang, B., Fang, J., Lang, J., Tian, G., Jiang, J., Zhu, T.F., 2014. Inhalable microorganisms in Beijing's PM_{2.5} and PM₁₀ pollutants during a severe smog event. *Environ Sci Technol* 48, 1499-1507.

Chen, P.-S., Li, C.-S.J.A.S., Technology, 2005. Sampling performance for bioaerosols by flow cytometry with fluorochrome. 39, 231-237.

- Conen, F., Morris, C.E., Leifeld, J., Yakutin, M.V., Alewell, C., 2011. Biological residues define the ice nucleation properties of soil dust. *Atmospheric Chemistry and Physics* 11, 9643-9648.
- Conen, F., Rodríguez, S., Hüglin, C., Henne, S., Herrmann, E., Bukowiecki, N., Alewell, C., 2015. Atmospheric ice nuclei at the high-altitude observatory Jungfraujoch, Switzerland. *Tellus B* 67.
- Constantinidou, H., Hirano, S., Baker, L., Upper, C., 1990. Atmospheric dispersal of ice nucleation-active bacteria: the role of rain. *Phytopathology* 80, 934-937.
- Creamean, J.M., Ault, A.P., White, A.B., Neiman, P.J., Ralph, F.M., Minnis, P., Prather, K.A., 2015. Impact of interannual variations in aerosol particle sources on orographic precipitation over California's Central Sierra Nevada. *Atmospheric Chemistry and Physics Discussions* 15, 931-964.
- Creamean, J.M., Suski, K.J., Rosenfeld, D., Cazorla, A., DeMott, P.J., Sullivan, R.C., White, A.B., Ralph, F.M., Minnis, P., Comstock, J.M., Tomlinson, J.M., Prather, K.A., 2013. Dust and biological aerosols from the Sahara and Asia influence precipitation in the western U.S. *Science* 339, 1572-1578.
- Daho, T., Vaitilingom, G., Sanogo, O., Ouiminga, S.K., Segda, B.G., Valette, J., Higelin, P., Koulidiati, J., 2012. Study of droplet vaporization of various vegetable oils and blends of domestic fuel oil–cottonseed oil under different ambient temperature conditions. *Biomass and Bioenergy* 46, 653-663.
- Delort, A.-M., Vaitilingom, M., Amato, P., Sancelme, M., Parazols, M., Mailhot, G., Laj, P., Deguillaume, L., 2010. A short overview of the microbial population in clouds: potential roles in atmospheric chemistry and nucleation processes. *Atmospheric Research* 98, 249-260.
- DeMott, P.J., Prenni, A.J., 2010. New directions: need for defining the numbers and sources of biological aerosols acting as ice nuclei. *Atmospheric Environment* 44, 1944-1945.
- Després, V., Nowoisky, J., Klose, M., Conrad, R., Andreae, M., Pöschl, U., 2007. Characterization of primary biogenic aerosol particles in urban, rural, and high-alpine air by DNA sequence and restriction fragment analysis of ribosomal RNA genes. *Biogeosciences* 4, 1127-1141.
- Du, R., Du, P., Lu, Z., Ren, W., Liang, Z., Qin, S., Li, Z., Wang, Y., Fu, P., 2017. Evidence for a missing source of efficient ice nuclei. *Scientific Reports* 7, 39673.
- Dueker, M.E., French, S., O'Mullan, G.D., 2018. Comparison of Bacterial Diversity in Air and Water of a Major Urban Center. 9.
- Durand, K.T.H., Mulenge, M.L., Burge, H.A., Seixas, Noah S., 2002. Effect of Sampling Time on the Culturability of Airborne Fungi and Bacteria Sampled by Filtration. *The Annals of Occupational Hygiene* 46, 113-118.
- Fan, C., Hu, W., Zhang, D., 2022. Calibration for number size distribution of bacterial cells measured with traditional size-segregated aerosol samplers. *Journal of Aerosol Science* 166,

106071.

Fan, C., Li, Y., Liu, P., Mu, F., Xie, Z., Lu, R., Qi, Y., Wang, B., Jin, C., 2019. Characteristics of airborne opportunistic pathogenic bacteria during autumn and winter in Xi'an, China. *Science of The Total Environment* 672, 834-845.

Fan, X.-B., Okada, K., Niimura, N., Kai, K., Arao, K., Shi, G.-Y., Qin, Y., Mitsuta, Y., 1996. Mineral particles collected in China and Japan during the same Asian dust-storm event. *Atmospheric Environment* 30, 347-351.

Fang, Z., Ouyang, Z., Zheng, H., Wang, X., Hu, L., 2007. Culturable airborne bacteria in outdoor environments in Beijing, China. *Microb Ecol* 54, 487-496.

Fenchel, T., Finlay, B.J., 2004. The ubiquity of small species: patterns of local and global diversity. *Bioscience* 54, 777-784.

Ferguson, R.M.W., Neath, C.E.E., Nasir, Z.A., Garcia-Alcega, S., Tyrrel, S., Coulon, F., Dumbrell, A.J., Colbeck, I., Whitby, C., 2021. Size fractionation of bioaerosol emissions from green-waste composting. *Environment International* 147, 106327.

Franzetti, A., Gandolfi, I., Gaspari, E., Ambrosini, R., Bestetti, G.J.A.m., *biotechnology*, 2011. Seasonal variability of bacteria in fine and coarse urban air particulate matter. 90, 745-753.

Fröhlich-Nowoisky, J., Kampf, C.J., Weber, B., Huffman, J.A., Pöhlker, C., Andreae, M.O., Lang-Yona, N., Burrows, S.M., Gunthe, S.S., Elbert, W., Su, H., Hoor, P., Thines, E., Hoffmann, T., Després, V.R., Pöschl, U., 2016. Bioaerosols in the Earth system: Climate, health, and ecosystem interactions. *Atmospheric Research* 182, 346-376.

Fröhlich-Nowoisky, J., Ruzene Nespoli, C., Pickersgill, D.A., Galand, P., Müller-Germann, I., Nunes, T., Gomes Cardoso, J., Almeida, S.M., Pio, C., Andreae, M.J.B., 2014a. Diversity and seasonal dynamics of airborne archaea. 11, 6067-6079.

Fröhlich-Nowoisky, J., Ruzene Nespoli, C., Pickersgill, D.A., Galand, P.E., Müller-Germann, I., Nunes, T., Gomes Cardoso, J., Almeida, S.M., Pio, C., Andreae, M.O., Conrad, R., Pöschl, U., Després, V.R., 2014b. Diversity and seasonal dynamics of airborne archaea. *Biogeosciences* 11, 6067-6079.

Fuzzi, S., Mandrioli, P., Perfetto, A., 1997. Fog droplets—an atmospheric source of secondary biological aerosol particles. *Atmospheric Environment* 31, 287-290.

Gabey, A.M., Gallagher, M.W., Whitehead, J., Dorsey, J.R., Kaye, P.H., Stanley, W.R., 2010. Measurements and comparison of primary biological aerosol above and below a tropical forest canopy using a dual channel fluorescence spectrometer. *Atmospheric Chemistry and Physics* 10, 4453-4466.

Gabey, A.M., Stanley, W.R., Gallagher, M.W., Kaye, P.H., 2011. The fluorescence properties of

aerosol larger than 0.8 μ m in urban and tropical rainforest locations. *Atmospheric Chemistry and Physics* 11, 5491-5504.

Gao, M., Qiu, T., Jia, R., Han, M., Song, Y., Wang, X., 2014. Concentration and size distribution of viable bioaerosols during non-haze and haze days in Beijing. *Environ Sci Pollut Res Int*.

Garcia, E., Hill, T.C.J., Prenni, A.J., DeMott, P.J., Franc, G.D., Kreidenweis, S.M., 2012. Biogenic ice nuclei in boundary layer air over two U.S. High Plains agricultural regions. *Journal of Geophysical Research: Atmospheres* 117, D18343.

Gong, J., Qi, J., E, B., Yin, Y., Gao, D., 2020. Concentration, viability and size distribution of bacteria in atmospheric bioaerosols under different types of pollution. *Environmental Pollution* 257, 113485.

Griffin, D.W., 2007. Atmospheric movement of microorganisms in clouds of desert dust and implications for human health. *Clin Microbiol Rev* 20, 459-477.

Griffin, D.W., Garrison, V.H., Herman, J.R., Shinn, E.A., 2001. African desert dust in the Caribbean atmosphere: microbiology and public health. *Aerobiologia* 17, 203-213.

Hairston, P.P., Ho, J., Quant, F.R., 1997. Design of an instrument for real-time detection of bioaerosols using simultaneous measurement of particle aerodynamic size and intrinsic fluorescence. *Journal of Aerosol Science* 28, 471-482.

Hara, K., Zhang, D., 2012. Bacterial abundance and viability in long-range transported dust. *Atmospheric Environment* 47, 20-25.

Hara, K., Zhang, D., Yamada, M., Matsusaki, H., Arizono, K., 2011. A detection of airborne particles carrying viable bacteria in an urban atmosphere of Japan. *Asian Journal of Atmospheric Environment* 5, 152-156.

Harrison, R.M., Jones, A.M., Biggins, P.D., Pomeroy, N., Cox, C.S., Kidd, S.P., Hobman, J.L., Brown, N.L., Beswick, A., 2005. Climate factors influencing bacterial count in background air samples. *Int J Biometeorol* 49, 167-178.

Herlihy, L.J., Galloway, J.N., Mills, A.L., 1987. Bacterial utilization of formic and acetic acid in rainwater. *Atmospheric Environment (1967)* 21, 2397-2402.

Hill, S.C., Doughty, D.C., Pan, Y.-L., Williamson, C., Santarpia, J.L., Hill, H.H., 2014. Fluorescence of bioaerosols: mathematical model including primary fluorescing and absorbing molecules in bacteria: errata. *Optics Express* 22, 22817.

Hu, W., Murata, K., Fan, C., Huang, S., Matsusaki, H., Fu, P., Zhang, D., 2020. Abundance and viability of particle-attached and free-floating bacteria in dusty and nondusty air. *Biogeosciences* 17, 4477-4487.

- Hu, W., Murata, K., Fukuyama, S., Kawai, Y., Oka, E., Uematsu, M., Zhang, D., 2017a. Concentration and Viability of Airborne Bacteria Over the Kuroshio Extension Region in the Northwestern Pacific Ocean: Data From Three Cruises. *Journal of Geophysical Research: Atmospheres* 122, 12892-12905.
- Hu, W., Murata, K., Horikawa, Y., Naganuma, A., Zhang, D., 2017b. Bacterial community composition in rainwater associated with synoptic weather in an area downwind of the Asian continent. *Sci Total Environ* 601-602, 1775-1784.
- Huffman, J., Treutlein, B., Pöschl, U., 2010. Fluorescent biological aerosol particle concentrations and size distributions measured with an Ultraviolet Aerodynamic Particle Sizer (UV-APS) in Central Europe. *Atmospheric Chemistry and Physics* 10, 3215-3233.
- Jaenicke, R., 2005. Abundance of cellular material and proteins in the atmosphere. *Science* 308, 73.
- Jensen, P.A., Schafer, M.P.J.N.m.o.a.m., 1998. Sampling and characterization of bioaerosols. 1, 82-112.
- Joly, M., Amato, P., Sancelme, M., Vinatier, V., Abrantes, M., Deguillaume, L., Delort, A.-M., 2015. Survival of microbial isolates from clouds toward simulated atmospheric stress factors. *Atmospheric Environment* 117, 92-98.
- Joly, M., Attard, E., Sancelme, M., Deguillaume, L., Guilbaud, C., Morris, C.E., Amato, P., Delort, A.-M., 2013. Ice nucleation activity of bacteria isolated from cloud water. *Atmospheric Environment* 70, 392-400.
- Kasprzyk, I., Walanus, A., 2014. Gamma, Gaussian and logistic distribution models for airborne pollen grains and fungal spore season dynamics. *Aerobiologia (Bologna)* 30, 369-383.
- Kaye, P.H., Stanley, W.R., Hirst, E., Foot, E.V., Baxter, K.L., Barrington, S.J., 2005. Single particle multichannel bio-aerosol fluorescence sensor. *Optics Express* 13, 3583-3593.
- Li, W., Liu, L., Xu, L., Zhang, J., Yuan, Q., Ding, X., Hu, W., Fu, P., Zhang, D., 2020. Overview of primary biological aerosol particles from a Chinese boreal forest: Insight into morphology, size, and mixing state at microscopic scale. *Science of The Total Environment* 719, 137520.
- Lighthart, B., 1997. The ecology of bacteria in the alfresco atmosphere. *FEMS Microbiology Ecology* 23, 263-274.
- Lighthart, B., 2000. Mini-review of the concentration variations found in the alfresco atmospheric bacterial populations. *Aerobiologia* 16, 7-16.
- Lighthart, B., Hiatt, V.E., Rossano Jr, A.T.J.J.o.t.A.P.C.A., 1971. The survival of airborne *Serratia marcescens* in urban concentrations of sulfur dioxide. 21, 639-642.

- Limpert, E., Burke, J., Galan, C., Trigo, M.d.M., West, J.S., Stahel, W.A., 2008. Data, not only in aerobiology: how normal is the normal distribution? *Aerobiologia* 24, 121-124.
- Lin, B., Ross, S.D., Prussin, A.J., Schmale, D.G., 2014. Seasonal associations and atmospheric transport distances of fungi in the genus *Fusarium* collected with unmanned aerial vehicles and ground-based sampling devices. *Atmospheric Environment* 94, 385-391.
- Lin, J.J., Noll, K.E., Holsen, T.M., 1994. Dry Deposition Velocities as a Function of Particle Size in the Ambient Atmosphere. *Aerosol Science and Technology* 20, 239-252.
- Mahowald, N., Albani, S., Kok, J.F., Engelstaeder, S., Scanza, R., Ward, D.S., Flanner, M.G., 2014. The size distribution of desert dust aerosols and its impact on the Earth system. *Aeolian Research* 15, 53-71.
- Maki, T., Susuki, S., Kobayashi, F., Kakikawa, M., Yamada, M., Higashi, T., Chen, B., Shi, G., Hong, C., Tobo, Y., 2008. Phylogenetic diversity and vertical distribution of a halobacterial community in the atmosphere of an Asian dust (KOSA) source region, Dunhuang City. *Air Quality, Atmosphere & Health* 1, 81-89.
- Mandrioli, P., Negrini, M.G., Cesari, G., Morgan, G., 1984. Evidence for long range transport of biological and anthropogenic aerosol particles in the atmosphere. *Grana* 23, 43-53.
- Maron, P.-A., Lejon, D.P.H., Carvalho, E., Bizet, K., Lemanceau, P., Ranjard, L., Mougel, C., 2005. Assessing genetic structure and diversity of airborne bacterial communities by DNA fingerprinting and 16S rDNA clone library. *Atmospheric Environment* 39, 3687-3695.
- Matthias-Maser, S., Brinkmann, J., Schneider, W., 1999. The size distribution of marine atmospheric aerosol with regard to primary biological aerosol particles over the South Atlantic Ocean. *Atmospheric Environment* 33, 3569-3575.
- Matthias-Maser, S., Jaenicke, R., 1995. The size distribution of primary biological aerosol particles with radii > 0.2 μ m in an urban/rural influenced region. *Atmospheric Research* 39, 279-286.
- Matthias-Maser, S., Jaenicke, R., 2000. The size distribution of primary biological aerosol particles in the multiphase atmosphere. *Aerobiologia* 16, 207-210.
- Mayol, E., Arrieta, J.M., Jimenez, M.A., Martinez-Asensio, A., Garcias-Bonet, N., Dachs, J., Gonzalez-Gaya, B., Royer, S.J., Benitez-Barrios, V.M., Fraile-Nuez, E., Duarte, C.M., 2017. Long-range transport of airborne microbes over the global tropical and subtropical ocean. *Nature communications* 8, 201.
- Michaud, A.B., Dore, J.E., Leslie, D., Lyons, W.B., Sands, D.C., Priscu, J.C., 2014. Biological ice nucleation initiates hailstone formation. *Journal of Geophysical Research: Atmospheres* 119, 12186-12197.
- Miteva, V.I., Brenchley, J.E., 2005. Detection and Isolation of Ultrasmall Microorganisms from a

120,000-Year-Old Greenland Glacier Ice Core. 71, 7806-7818.

Möhler, O., DeMott, P., Vali, G., Levin, Z., 2007a. Microbiology and atmospheric processes: the role of biological particles in cloud physics. *Biogeosciences* 4, 1059-1071.

Möhler, O., DeMott, P.J., Vali, G., Levin, Z., 2007b. Microbiology and atmospheric processes: the role of biological particles in cloud physics. *Biogeosciences* 4, 1059-1071.

Monteil, C.L., Bardin, M., Morris, C.E., 2014. Features of air masses associated with the deposition of *Pseudomonas syringae* and *Botrytis cinerea* by rain and snowfall. *ISME J* 8, 2290-2304.

Montero, A., Dueker, M.E., O'Mullan, G.D., 2016. Culturable bioaerosols along an urban waterfront are primarily associated with coarse particles. *PeerJ* 4, e2827.

Moore, R.A., Hanlon, R., Powers, C., Schmale, D.G., Christner, B.C., 2020. Scavenging of Sub-Micron to Micron-Sized Microbial Aerosols during Simulated Rainfall. *Atmosphere* 11, 80.

Morris, C.E., Conen, F., Alex Huffman, J., Phillips, V., Poschl, U., Sands, D.C., 2014. Bioprecipitation: a feedback cycle linking earth history, ecosystem dynamics and land use through biological ice nucleators in the atmosphere. *Glob Chang Biol* 20, 341-351.

Murata, K., Zhang, D., 2013. Applicability of LIVE/DEAD BacLight Stain with Glutaraldehyde Fixation for the Measurement of Bacterial Cell Concentration and Viability in the Air. *Aerosol and Air Quality Research* 13, 1755-1767.

Murata, K., Zhang, D., 2014. Transport of bacterial cells toward the Pacific in Northern Hemisphere westerly winds. *Atmospheric Environment* 87, 138-145.

Murata, K., Zhang, D., 2016. Concentration of bacterial aerosols in response to synoptic weather and land-sea breeze at a seaside site downwind of the Asian continent. *Journal of Geophysical Research: Atmospheres* 121, 11636-11647.

Okada, K., Kai, K., 2004. Atmospheric mineral particles collected at Qira in the Taklamakan Desert, China. *Atmospheric Environment* 38, 6927-6935.

Polymenakou, P.N., Mandalakis, M., Stephanou, E.G., Tselepidis, A., 2008. Particle size distribution of airborne microorganisms and pathogens during an Intense African dust event in the eastern Mediterranean. *Environ Health Perspect* 116, 292-296.

Pöschl, U., Martin, S.T., Sinha, B., Chen, Q., Gunthe, S.S., Huffman, J.A., Borrmann, S., Farmer, D.K., Garland, R.M., Helas, G., Jimenez, J.L., King, S.M., Manzi, A., Mikhailov, E., Pauliquevis, T., Petters, M.D., Prenni, A.J., Roldin, P., Rose, D., Schneider, J., Su, H., Zorn, S.R., Artaxo, P., Andreae, M.O., 2010. Rainforest aerosols as biogenic nuclei of clouds and precipitation in the Amazon. *Science* 329, 1513-1516.

Pratt, K.A., DeMott, P.J., French, J.R., Wang, Z., Westphal, D.L., Heymsfield, A.J., Twohy, C.H.,

- Prenni, A.J., Prather, K.A., 2009. In situ detection of biological particles in cloud ice-crystals. *Nature Geoscience* 2, 398-401.
- Prospero, J.M., Blades, E., Mathison, G., Naidu, R., 2005. Interhemispheric transport of viable fungi and bacteria from Africa to the Caribbean with soil dust. *Aerobiologia* 21, 1-19.
- Raisi, L., Aleksandropoulou, V., Lazaridis, M., Katsivela, E., 2013. Size distribution of viable, cultivable, airborne microbes and their relationship to particulate matter concentrations and meteorological conditions in a Mediterranean site. *Aerobiologia* 29, 233-248.
- Raupach, T.H., Berne, A., 2015. Correction of raindrop size distributions measured by Parsivel disdrometers, using a two-dimensional video disdrometer as a reference. *Atmospheric Measurement Techniques* 8, 343-365.
- Raynor, G.S., Hayes, J.V., Ogden, E.C., 1974. Mesoscale Transport and Dispersion of Airborne Pollens %J *Journal of Applied Meteorology and Climatology*. 13, 87-95.
- Reinmuth-Selzle, K., Kampf, C.J., Lucas, K., Lang-Yona, N., Frohlich-Nowoisky, J., Shiraiwa, M., Lakey, P.S.J., Lai, S., Liu, F., Kunert, A.T., Ziegler, K., Shen, F., Sgarbanti, R., Weber, B., Bellinghausen, I., Saloga, J., Weller, M.G., Duschl, A., Schuppan, D., Poschl, U., 2017. Air Pollution and Climate Change Effects on Allergies in the Anthropocene: Abundance, Interaction, and Modification of Allergens and Adjuvants. *Environ Sci Technol* 51, 4119-4141.
- Savage, N.J., Krentz, C.E., Könemann, T., Han, T.T., Mainelis, G., Pöhlker, C., Huffman, J.A., 2017. Systematic characterization and fluorescence threshold strategies for the wideband integrated bioaerosol sensor (WIBS) using size-resolved biological and interfering particles. *Atmospheric Measurement Techniques* 10, 4279-4302.
- Schnell, R., Vali, G.J.J.o.A.S., 1976. Biogenic ice nuclei: Part I. Terrestrial and marine sources. *Journal of Atmospheric Sciences* 33, 1554-1564.
- Schuerger, A.C., Smith, D.J., Griffin, D.W., Jaffe, D.A., Wawrik, B., Burrows, S.M., Christner, B.C., Gonzalez-Martin, C., Lipp, E.K., Schmale Iii, D.G., Yu, H., 2018. Science questions and knowledge gaps to study microbial transport and survival in Asian and African dust plumes reaching North America. *Aerobiologia* 34, 425-435.
- Shaffer, B.T., Lighthart, B., 1997. Survey of culturable airborne bacteria at four diverse locations in Oregon: urban, rural, forest, and coastal. *Microbial Ecology* 34, 167-177.
- Shi, J., Wang, N., Gao, H., Baker, A.R., Yao, X., Zhang, D., 2019. Phosphorus solubility in aerosol particles related to particle sources and atmospheric acidification in Asian continental outflow. *Atmospheric Chemistry and Physics* 19, 847-860.
- Smets, W., Moretti, S., Denys, S., Lebeer, S., 2016. Airborne bacteria in the atmosphere: presence, purpose, and potential. *Atmospheric Environment* 139, 214-221.

- Smith, D.J., 2013. Microbes in the Upper Atmosphere and Unique Opportunities for Astrobiology Research. *Astrobiology* 13, 981-990.
- Smith, D.J., Jaffe, D.A., Birmele, M.N., Griffin, D.W., Schuerger, A.C., Hee, J., Roberts, M.S., 2012a. Free Tropospheric Transport of Microorganisms from Asia to North America. *Microbial Ecology* 64, 973-985.
- Smith, D.J., Jaffe, D.A., Birmele, M.N., Griffin, D.W., Schuerger, A.C., Hee, J., Roberts, M.S., 2012b. Free tropospheric transport of microorganisms from Asia to North America. *Microbiome Ecology* 64, 973-985.
- Speight, S., Hallis, B., Bennett, A., Benbough, J.J.J.o.a.s., 1997. Enzyme-linked immunosorbent assay for the detection of airborne microorganisms used in biotechnology. *Journal of Aerosol Science* 28, 483-492.
- Tobo, Y., Adachi, K., DeMott, P.J., Hill, T.C.J., Hamilton, D.S., Mahowald, N.M., Nagatsuka, N., Ohata, S., Uetake, J., Kondo, Y., Koike, M., 2019. Glacially sourced dust as a potentially significant source of ice nucleating particles. *Nature Geoscience* 12, 253-258.
- Tobo, Y., Prenni, A.J., DeMott, P.J., Huffman, J.A., McCluskey, C.S., Tian, G., Pöhlker, C., Pöschl, U., Kreidenweis, S.M., 2013. Biological aerosol particles as a key determinant of ice nuclei populations in a forest ecosystem. *Journal of Geophysical Research: Atmospheres* 118, 10,100-110,110.
- Tong, Y., Lighthart, B., 2000. The Annual Bacterial Particle Concentration and Size Distribution in the Ambient Atmosphere in a Rural Area of the Willamette Valley, Oregon. *Aerosol Science and Technology* 32, 393-403.
- Uno, I., Eguchi, K., Yumimoto, K., Takemura, T., Shimizu, A., Uematsu, M., Liu, Z., Wang, Z., Hara, Y., Sugimoto, N., 2009. Asian dust transported one full circuit around the globe. *Nature Geoscience* 2, 557-560.
- Väitilingom, M., Deguillaume, L., Vinatier, V., Sancelme, M., Amato, P., Chaumerliac, N., Delort, A.M., 2013. Potential impact of microbial activity on the oxidant capacity and organic carbon budget in clouds. *Proceedings of the National Academic Science* 110, 559-564.
- Whitman, W.B., Coleman, D.C., Wiebe, W.J.J.P.o.t.N.A.o.S., 1998. Prokaryotes: the unseen majority. 95, 6578-6583.
- Wilkinson, D.M., Koumoutsaris, S., Mitchell, E.A.D., Bey, I., 2012. Modelling the effect of size on the aerial dispersal of microorganisms. *Journal of Biogeography* 39, 89-97.
- Wilson, T.W., Ladino, L.A., Alpert, P.A., Breckels, M.N., Brooks, I.M., Browse, J., Burrows, S.M., Carslaw, K.S., Huffman, J.A., Judd, C., Kilhau, W.P., Mason, R.H., McFiggans, G., Miller, L.A., Nájera, J.J., Polishchuk, E., Rae, S., Schiller, C.L., Si, M., Temprado, J.V., Whale, T.F., Wong,

- J.P.S., Wurl, O., Yakobi-Hancock, J.D., Abbatt, J.P.D., Aller, J.Y., Bertram, A.K., Knopf, D.A., Murray, B.J., 2015. A marine biogenic source of atmospheric ice-nucleating particles. *Nature* 525, 234-238.
- Woo, C., Yamamoto, N., 2020. Falling bacterial communities from the atmosphere. *Environmental Microbiome* 15, 22.
- Xu, S., Ren, L., Lang, Y., Hou, S., Ren, H., Wei, L., Wu, L., Deng, J., Hu, W., Pan, X., Sun, Y., Wang, Z., Su, H., Cheng, Y., Fu, P., 2020. Molecular markers of biomass burning and primary biological aerosols in urban Beijing: size distribution and seasonal variation. *Atmos. Chem. Phys.* 20, 3623-3644.
- Xu, Z., Wei, K., Wu, Y., Shen, F., Chen, Q., Li, M., Yao, M., 2013. Enhancing Bioaerosol Sampling by Andersen Impactors Using Mineral-Oil-Spread Agar Plate. *PLOS ONE* 8, e56896.
- Xu, Z., Wu, Y., Shen, F., Chen, Q., Tan, M., Yao, M., 2011. Bioaerosol science, technology, and engineering: past, present, and future. *Aerosol Science and Technology* 45, 1337-1349.
- Yamaguchi, N., Ichijo, T., Baba, T., Nasu, M., 2014. Long-range Transportation of Bacterial Cells by Asian Dust. *Genes and Environment* 36, 145-151.
- Yang, L., Shen, Z., Wang, D., Wei, J., Wang, X., Sun, J., Xu, H., Cao, J., 2021. Diurnal Variations of Size-Resolved Bioaerosols During Autumn and Winter Over a Semi-Arid Megacity in Northwest China. *Geohealth* 5, e2021GH000411.
- Yao, M., 2018. Reprint of bioaerosol: A bridge and opportunity for many scientific research fields. *Journal of Aerosol Science* 119, 91-96.
- Yao, M., Mainelis, G., 2007. Analysis of portable impactor performance for enumeration of viable bioaerosols. *Journal of Occupational and Environmental Hygiene* 4, 514-524.
- Yin, Y., Qi, J., Gong, J., Gao, D., 2021. Distribution of bacterial concentration and viability in atmospheric aerosols under various weather conditions in the coastal region of China. *Science of The Total Environment* 795, 148713.
- Yue, S., Ren, H., Fan, S., Wei, L., Zhao, J., Bao, M., Hou, S., Zhan, J., Zhao, W., Ren, L., Kang, M., Li, L., Zhang, Y., Sun, Y., Wang, Z., Fu, P., 2017. High abundance of fluorescent biological aerosol particles in winter in Beijing, China. *ACS Earth and Space Chemistry* 1, 493-502.
- Zhang, D., Iwasaka, Y., Shi, G., Zang, J., Matsuki, A., Trochkin, D., 2003. Mixture state and size of Asian dust particles collected at southwestern Japan in spring 2000. *Journal of Geophysical Research: Atmospheres* 108, 4760.
- Zhang, D., Shi, G.-Y., Iwasaka, Y., Hu, M., 2000. Mixture of sulfate and nitrate in coastal atmospheric aerosols: individual particle studies in Qingdao (36° 04' N, 120° 21' E), China. *Atmospheric Environment* 34, 2669-2679.

Zweifel, U.L., Hagström, Å., Holmfeldt, K., Thyraug, R., Geels, C., Frohn, L.M., Skjøth, C.A., Karlson, U.G., 2012. High bacterial 16S rRNA gene diversity above the atmospheric boundary layer. *Aerobiologia* 28, 481-498.